GHGSat Methane Emission Data: Technical Guide

Version 1.0

Satellite Applications Catapult

November 2023

We work with

Summary

This Technical Guide has been written by Satellite Applications Catapult to assist participants of the 2023-2024 GHGSat Methane Emission Data Project, access and use the GHGSat Methane Monitoring Data Archive via the SPECTRA portal. Participants are reminded that the GHGSat Methane Emissions Data Set provided through the project may only be used for research and development and not used for commercial purposes.

Acknowledgements

The Satellite Applications Catapult would like to thank the UK Space Agency for supporting this initiative, and the other contributors including the Ordinance Survey and the International Methane Emissions Observatory (IMEO) for their input.

Updates

This document is expected to be amended as updates are made to the SPECTRA platform and data availability. If something is unclear in the document or appears to have changed, please raise your query raise with the team by emailing: ch4.data@sa.catapult.org.uk

Version	Date	Editor	Amendment (page number and description of edit)
1.0	November 2023	Satellite Applications Catapult	Release of Technical Guide

Table of Contents

1. Introduction

GHGSat Methane Monitoring Data is provided in collaboration by the GHGSat, Satellite Applications Catapult (SAC), the Department for Environment, Food, and Rural Affairs (DEFRA), and the Ordinance Survey (OS) under a project funded by the UK Space Agency (UKSA). This dataset is being provided to UK based organisations, via the GHGSat's SPECTRA Data Portal, to promote innovation in the monitoring of methane emissions. This data is accessed through *GHGSat's SPECTRA Data Portal*. This technical guide will provide instructions on how to access the portal, search and download the data. A brief description of the data and how it is collected is also given, while references to more detailed explanations are also provided.

Why is methane (CH_4) important?

Methane is a potent greenhouse gas whose global mean concentration reached 1.92 ppm in 2023, an increase of 16% over the past four decades *(NOAA)*. While CH_4 concentrations are significantly smaller than CO_2 (423.68 ppm in 2023 – NOAA), its molecular structure makes it far more effective at trapping reflected thermal radiation, with a greenhouse potential ~85 times higher than CO_2 over a 20 year cycle *(IPCC 2023).* Accordingly, CH_4 constitutes 19% of the combined effective radiative forcing (ERF) *(Myhre et al., 2013)*, with well-mixed methane (chemical alterations to atmospheric ozone and halocarbons) providing a ERF of 1.19 [0.81 to 1.58] W m-2 (relative to 1750), second only to CO_2 (3.9 ± 0.5 Wm–2) (*Figure 1-1)*.

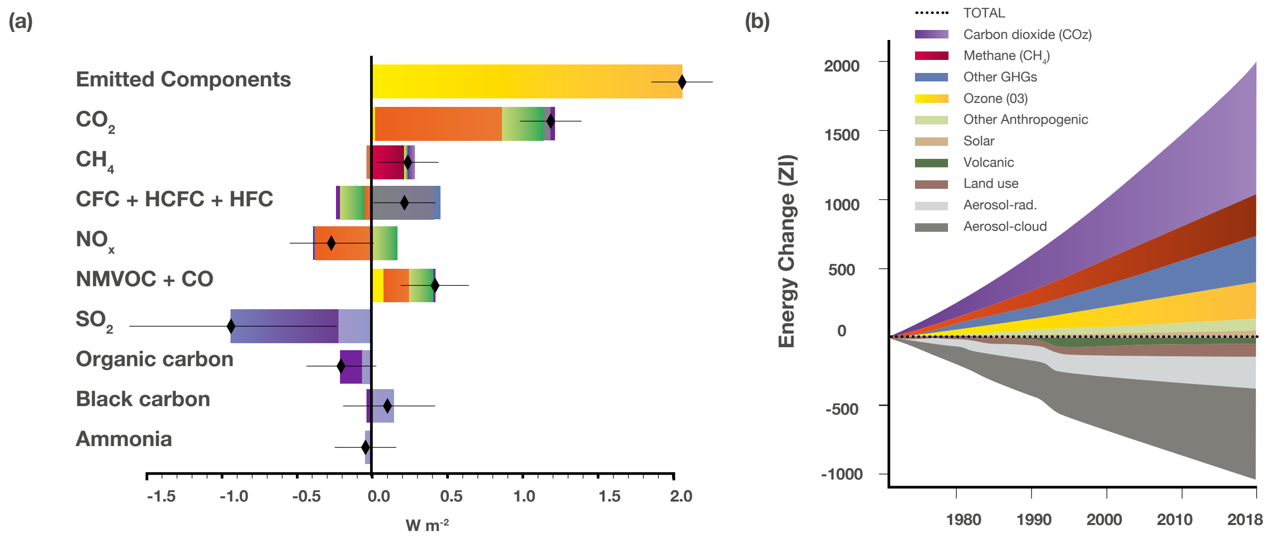

Figure 1-1: Climate change through effective radiative forcing (ERF) described by a) emitted contributions to ERF, estimated by the Coupled Model Intercomparison Project Phase 6 (CMIP6) models(5–95% error bars showing uncertainties); and b) estimates of the net cumulative energy change (ZJ = 1021 Joules) for the period 1971–2018 by all components, net forcing described by dashed black line. Source IPCC Report 2022

The global climate crisis requires states and industries to take rapid action to alter the trajectory of anthropogenic induced climate change. Reducing methane emissions is key to that target, as with a relatively short atmospheric lifetime of ten years (CO_2 = 300 -1000 years), changes in the volume and frequency of methane emissions will have a significant effect on the near-term warming rate *(Johannsson et al., 2008)*.

Methane emissions occur globally, with many anthropogenic point sources originating from several key industries, including:

- **Drilling/mining:** including energy markets: oil/gas facilities and coal mines (open and vented) (*Chen et al., 2022*; *Ialongo et al., 2021*) and mineral extraction: metallurgical coal *(for steel production)*.
- **Agriculture:** enteric fermentation, manure management, rice cultivation, and residue burning

(*Smith et al., 2021*; *Vechi et al., 2022*; *Kozicka et al., 2023*).

- **Waste disposal and treatment:** solid waste landfills (*Scheutz et al., 2022*) / wastewater treatment plants (*Wang et al., 2021*; *Bai et al., 2023*).

Studies have shown 60-90% of all methane emissions originate from a relatively small fraction of point sources, each producing flux (Q) in excess of 100 kg hr-1 (*Duren et al., 2019*).

The unique monitoring capabilities of earth observation (EO) satellites provide the only means to regularly monitor methane emissions at a global scale. Global missions, such as the *TROPOspheric Monitoring Instrument* (TROPOMI), aboard Copernicus' Sentinel-5p satellite, and the Greenhouse Gases Observing SATellite (GOSAT) (*Figure 1-2)* have provided regional maps of methane concentrations since 2017. Through these coarse resolution (> 7 km) daily maps, we have begun to understand where large concentrations of methane regularly occur. Yet, to better understand the causes of these emissions, finer resolution, targeted observations are required.

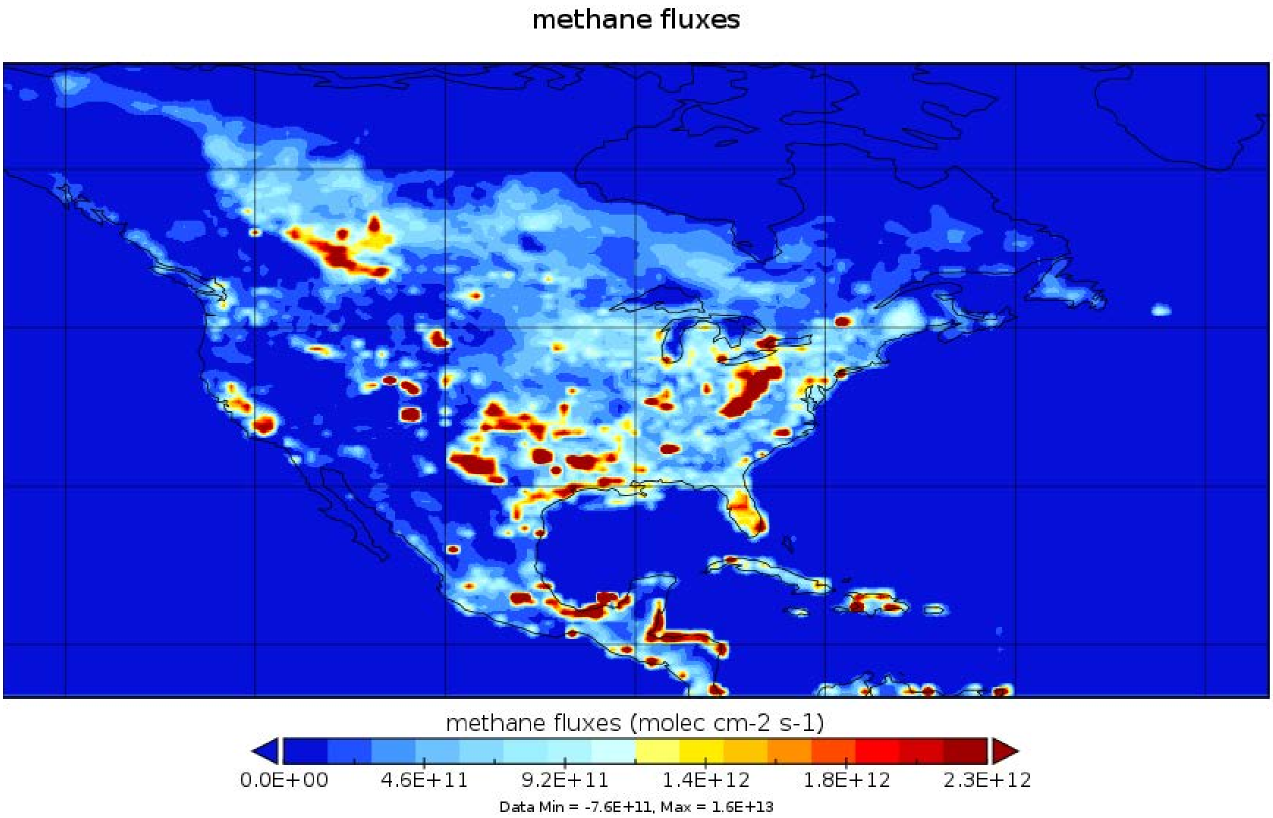

Figure 1-2: *Example methane emission measuring mission across north America using Greenhouse Gases Observing SATellite (GOSAT), observing methane emissions with a spatial resolution of 10 km. These types of data have improved our understanding of large-scale methane emissions; however, the resolution is too coarse to resolve facility scale sources of emissions. Source: NASA EarthData*

2. GHGSat constellation and data

GHGSat's constellation of nine (eleven expected by the end of 2023) methane monitoring satellites operate in a 500 km polar orbit, with the potential for daily monitoring of tasked target locations. The wide-angle Fabry Perot (WAF-P) imaging spectrometer has a spatial resolution of ~25 m and an observation field of view of approximately 12 km^2, providing both the resolution detail to define facility-scale features and the spatial scale to observe the full extent of the plume. This method has a detection threshold of CH_4 100 kg/hr for wind speed u=3 m/s.

By describing the total downwind emission plume, this data complements stationary ground-based systems, providing industry stakeholders and policy makers with the ability to accurately monitor total methane emissions from point (chimney or vent) and diffuse (landfill or open-pit mine) sources.

Mission highlights 2022

During 2022, the six satellites of the GHGSat constellation monitored over 500K locations and facilities worldwide, covering an area of 2 M km^2, measuring the equivalent of 179 MMT of CO_2 (CO_{2e}), which is equal to the emissions of 38.6 million cars driving for a year.

69% of all emissions were attributed to the extraction of fossil fuels (53% oil and gas / 16% coal). Other sources included, agriculture, landfills and naturally occurring methane, such as mud volcanos.

Oil and Gas detections revealed critical information, including persistent emissions from oil pipelines, flare stacks and storage tanks, helping industry stakeholders identify areas for maintenance and further monitoring. In the US, more than half of all emissions occurred in the Permian Basin, where the Oil and Gas industry is working with GHGSat and the Environmental Protection Agency (EPA) to create and maintain performance targets for known 'super emitter' sites (>100 kg/h).

GHGSat datasets were used in collaboration around the globe *(Maasakkers et al. 2022)*. The large-scale coverage of TROPOMI identified areas of high methane concentration, while the high-resolution GHGSat data would identify specific sources around landfill sites. These complementary data demonstrated how large emissions (3-29 t $hour^{-1}$) in Buenos Aires, Delhi, Lahore, and Mumbai contribute up to 50% of the cities' methane emissions.

The WAF-P imaging spectrometer

The WAF-P imaging spectrometer operates in the shortwave infrared (SWIR) between 1630 – 1675 nm where methane, CO_2, and water vapour gases are known to absorb reflected solar radiation. The atmospheric spectral absorption characteristic of a given location are observed by multiple (~200) overlapping images, taken as the satellite traverses its orbital track *(Figure 2-1)(a),(b)*.

For each image, the circular aperture captures the absorption spectrum in the form of spectral rings (dark band = high absorption), where the radius from the centre observes different wavelengths due to the angle-dependent Fabry-Perot transmission spectrum *(Figure 2-1)*. By focusing on a narrow band of SWIR, the sensor has a high spectral sampling frequency of 0.0001 - 0.1 nm (finer sampling occurs nearer to the centre of the detector aperture).

As the imager traverses the scene, the target location is (optimally) positioned in the centre of the image (orange x in *(Figure 2-1)(a),(b)* allowing each sequential image to capture absorption rates at different wavelengths (defined by radial position from the centre) for the same location. These captures combine to complete the spectral absorption profile between 1630 and 1675nm *(Figure 2-1)(c),(d)*.

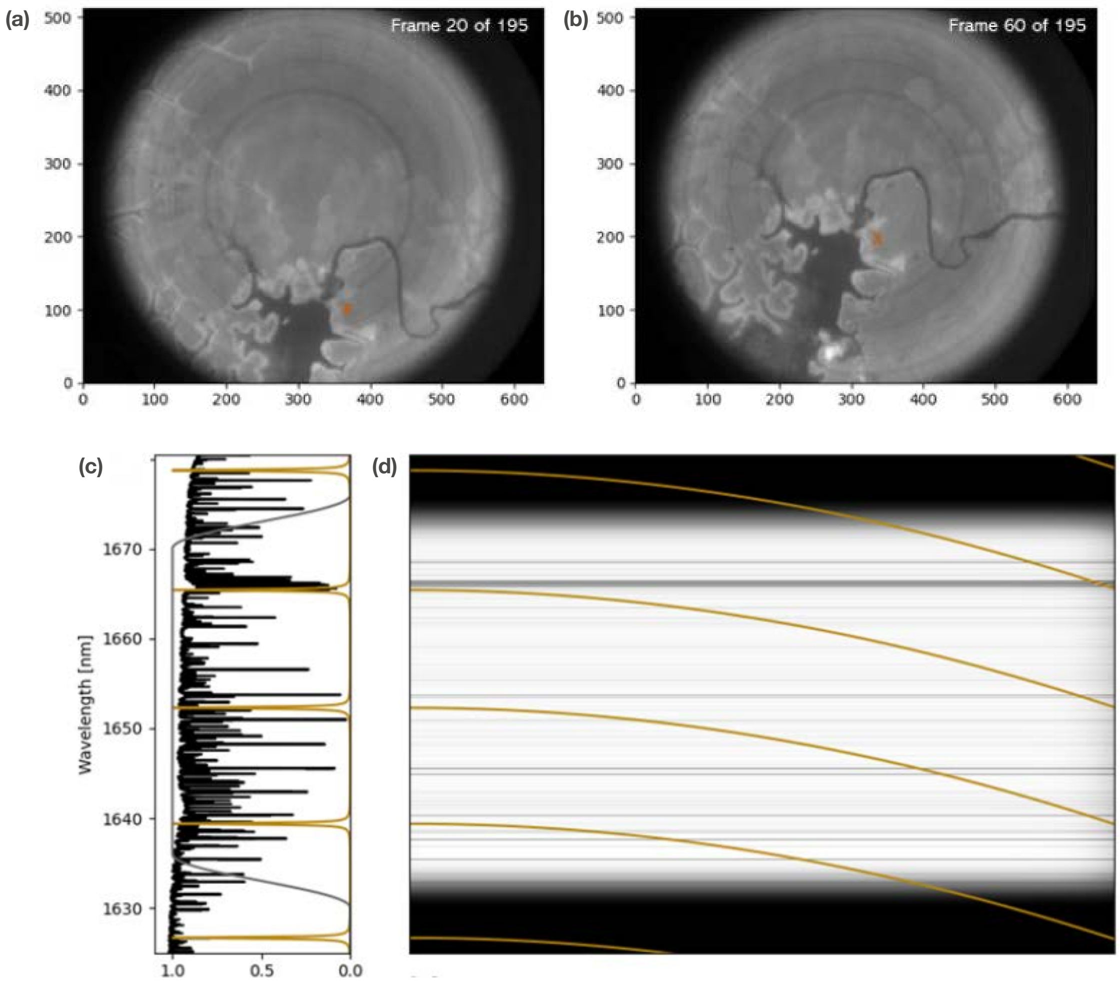

Figure 2-1: *Example of WAF-P imaging spectrometer image collection, where (a) and (b) show a selection of frames over the Lom Pangar hydroelectric reservoir in Cameroon (April 20th, 2017). Orange "x" denotes a tracked target in each frame, where its radial position describes the absorption characterisitcs (dark = high absorption, light = low absorption) at specific wavelengths (1630 nm center = 1675 nm outer rings) within the Fabry Perot (F-P) spectrum (light grey in (c)). Each pixel (described by axes) represents a 24 x 24 m2 area on the ground. c) Collated frame observations complete F-P absorption spectrum within the SWIR transmission window (1630-1675 nm) as normalized top-of-atmosphere spectral radiance (TOASR). The location of the F-P transmission peaks are shown as a function of radius (gold lines) overlaid on the normalized TOASR (grey-scale background image). The horizontal dark bands at the top and bottom of (d) illustrate the range of wavelengths within the F-P transmission window. Source: Jervis et al., 2021*

Methane emission concentration retrieval

Normalized top-of-atmosphere spectral radiance (TOASR) profiles are compared to a forward model of atmospheric composition, which simulates background conditions by considering variability in surface albedo (acquired from Landsat-8) and closest-in-time background gas concentrations, including methane (CH_4), carbon dioxide (CO_2), and water vapour vertical column densities (mol m^{-2}) – as described by the Atmospheric Infrared Sounder (AIRS) instrument. The residual difference in the TOASR absorption profiles and forward model projections are converted into methane concentrations per pixel using the Beer-Lambert law:

$$A = abc$$

where the measured absorption (A) equals the molecular absorption rate at a given wavelength (a) multiplied by the pathlength (b), and the count (c) of molecules in the sample. Where a and b are known, and therefore fixed, the residual absorption is directly related to c (i.e., the number of methane molecules observed (mol m^{-2}) *(Figure 2-2)* and is converted into parts per billion volume (ppbv) above background emission. *(Figure 2-2)*. A full 12 km scene consists of around 200,000 ground cells (pixel) and is presented as an abundance image (*Figure 2-3 (b)*. These are assessed using AI and validated by trained operators to identify emission plumes. Plumes are analysed to derive an emission source rate (Q), which estimate the mass of methane released per hour (kg/hr):

$$Q = \frac{U_{eff}(U) \times IME}{L}$$

Where total plume concentration = Integrated Mass Enhancement (IME), multiplied by effective wind speed (Ueff(U)) divided by the plume length (L) (*Varon et al., 2018*).

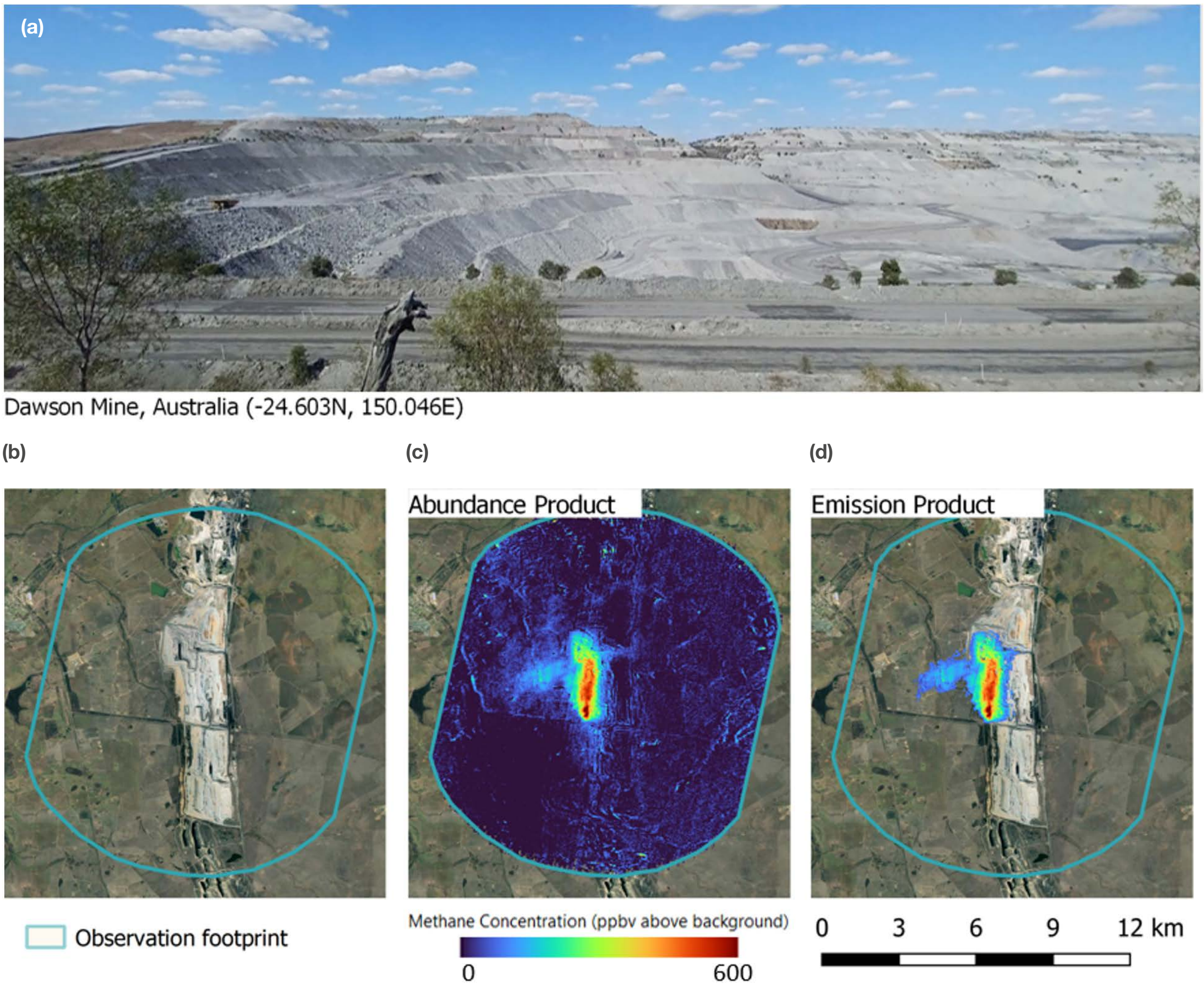

Figure 2-2: *Example of GHG Methane Products over Dawson Mine, Australia, August 2022, including b) the observation field of view footprint, c) the full Abundance Product, and d) the extracted emission plume data. Emission values present a parts per volume against background methane concentrations. a) image of the Dawson Mine. Digital image. Heather Jenkins https://www.google.com/maps/place/Dawson+Mine.*

Source rate error:

When estimating the source rate, there are inherent uncertainties due to the complexity of the process and the limitations of available data and models. The source rate error is a measure of this uncertainty. It is expressed as the standard deviation, which indicates the average amount of potential deviation or spread from the estimated source rate.

Any errors occur mainly within the forward model, CH_4 retrieval estimation and wind speed. Typically, the model error is about 7%, the measurement error is about 10%, with wind speed error (10% and 65%) typically dominating the source rate error. The final error is the combination of these three errors (addition in quadrature). For full product description of the WAF-P imaging spectrometer, see *Jervis et al., 2021*. For an independent description of data performance and errors, see *Sherwin et al., 2023*.

3. Data availability

Through the UKSA Data Provision Project, eligible users will have access to a large subset of GHGSat data. These data cover a range of sites of interest across multiple industrial sectors.

Sites of interest were selected across multiple industries around the globe, using past studies to identify potential sites where methane emissions are expected to occur. These sites were compared to GHGSat archive imagery, with a final selection of locations based on there being a minimum of one identified emission plume. For each selected location, all detected emission plumes between January 2021 and March 2023 are included in final data selection. All archive observations over the UK are also provided.

Initial data delivery: Data types and geographical distribution

The initial dataset was delivered at the onset of the project, including measurements from 1,337 satellite observations across 424 specific sites across the globe *(Figure 3-1)*. These data include 1,546 individually identified emission plumes e.g., (*Figure 2-3)* and 443 full scene (12 km^2) background methane abundance data e.g., (*Figure 2-3)*.

As the project progresses further emission and abundance data will be added to the archive. There are also opportunities for participants to task an observation of an area of interest.

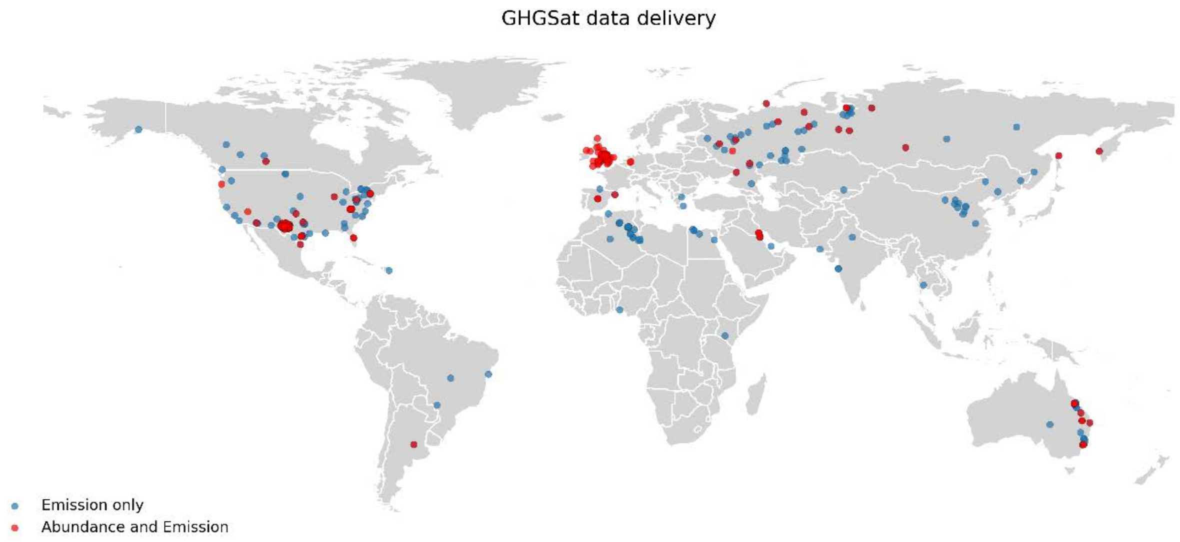

Figure 3-1: *Distribution of GHGSat Methane emission and abundance concentration data across the world.*

(Figure 3-2)(a),(b), shows the emission data distribution by continent. North America has the largest number of observation locations (231), followed by Europe (79), with the fewest in South America (4). From these locations, North America (524) produces the largest number of individual plumes, followed by Asia (400), Africa (243), Australasia (211), and Europe (158), with the fewest observed in South America (10).

(Figure 3-2)(c),(d), shows the distribution of abundence data by continent. North America has the largest number of locations with abundance data (82), followed by Europe (56), Asia (13), Australasia (9), and South America (1). There are no abundence data in Africa. From these locations, Europe produces the largest number of observations (176), followed by North America (124), Asia (54), Australasia (45), with the fewest coming from South America (44).

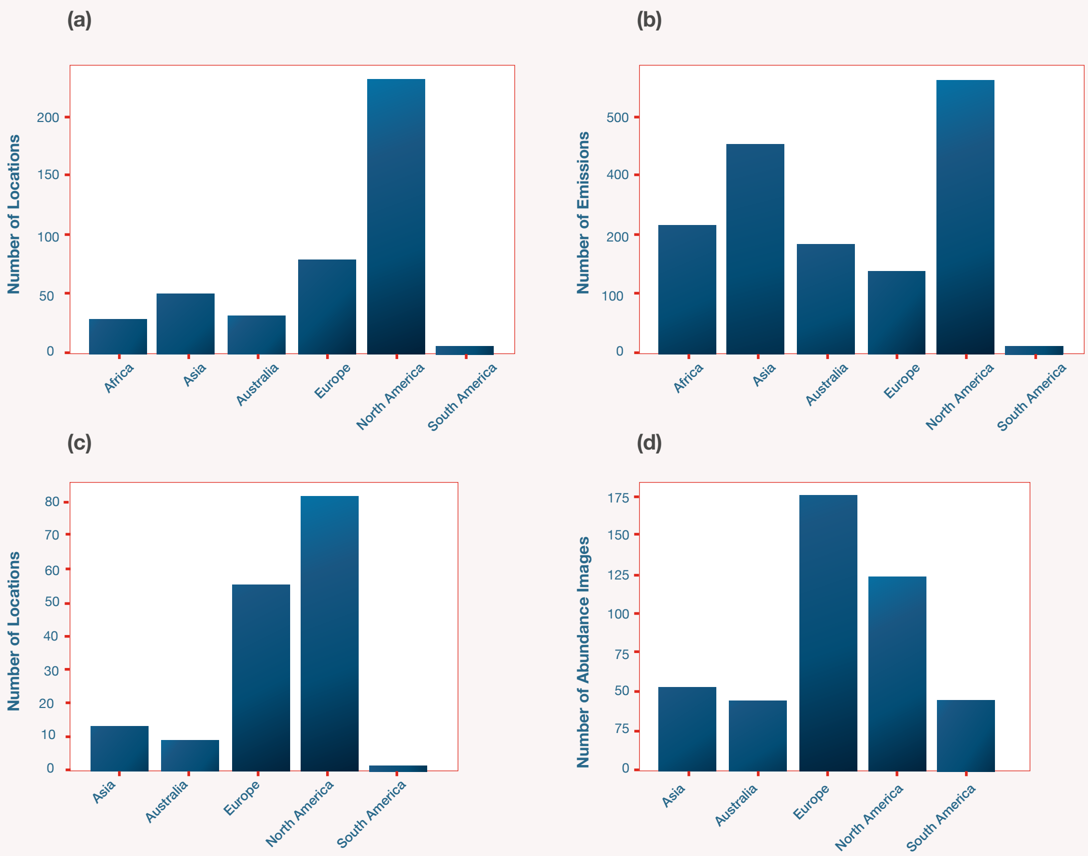

__Figure 3-2:__ Number of locations and observations of GHGSat methane emission and abundance concentration data by continent.

Observation frequency

Across the selected sites, the 1,337 satellite observations occur at different temporal frequencies since November 2020 (*Figure 3-3*). There was an average of 29.8 observations per month between November 2020 and May 2022, this increased to 75.7 observations per month following the *launch of three new satellites*, doubling the existing constellation. Similarly, the average number of detected emission plumes increased from 29.9 per month pre May 2022 to 94.2 since May 2022. Observations peaked in January 2023 (102 satellite observations), while emission plume detections peaked in March 2023 (132).

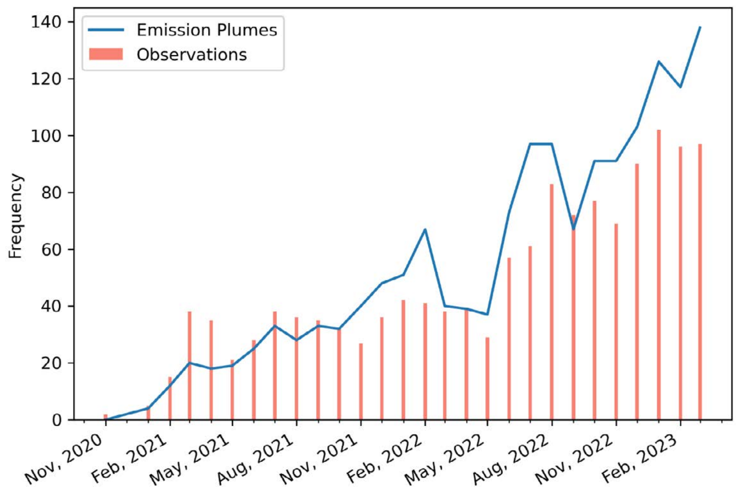

__Figure 3-3:__ Frequency of satellite observations and subsequent emission plume detections since November 2020.

Industry sectors

The data allocation has been selected to cover a range of industries, including:

Agriculture

- Livestock farming
- Abattoirs

Extractive industries

- Coal and mineral mining
- Oil and Gas drilling and pipelines
- Flare stack, excess gas burning

Landfills

- Known large landfill sites designated by region (EU, USA, Global)
- European sites also include wastewater treatement facilities

Observations and emission data

Oil and gas has the largest proportion of locations (62.5%), while the additional flare stack sites in Algeria and Egypt increase this proportion to 68.9% *(Figure 3-4)*. Oil and gas locations are predominantly in Russia, while other sites exist in North America, the Middle East, Australia, and North Africa *(Figure 3-5).* These sites cover 51.1% of all satellite observations and 52.9% of emission plumes (824 individual plumes). UK data cover the second largest number of sites, these data are covered in the UK Site section. Landfills cover 10% of all sites, including 24 in North America (5.7% of all sites), 10 in Europe (2.4%), and 8 (1.9%) in other global locations (Caribbean islands, Africa, and Asia). These locations provide 21.4% of satellite observations and 21.1% of the identified emission plumes. Mining sites cover 9.5% of all locations, including 13 coal mines in China (3.1%), and 27 mines in Australia (6.4%) *(Figure 3-5)*. These sites provide 11.6% of satellite observations and 21.8% (338) of emission plumes. Agriculture provides 1.95% of all observed locations. These include two abattoirs (0.5%), one each in North America and Australia, and six livestock sites (1.4%) including areas in South America, North America, and SE Asia. These sites cover 7.4% of all satellite observations, and 5.4% of emissions.

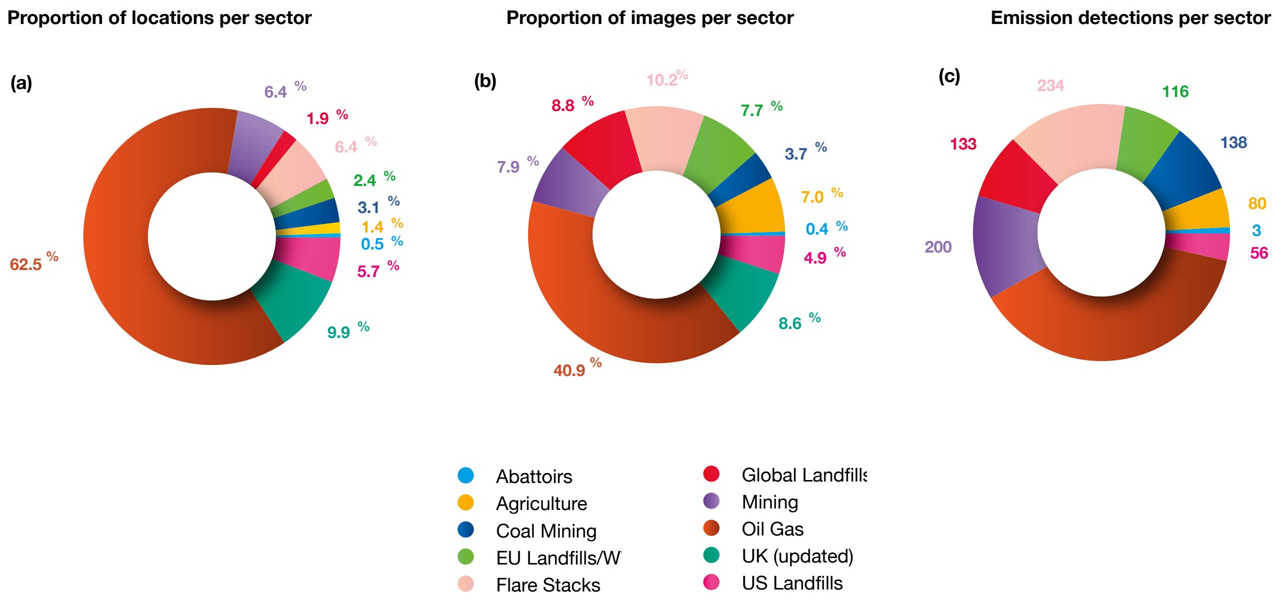

Figure 3-4: GHGSat data statistics for sector and location distribution.

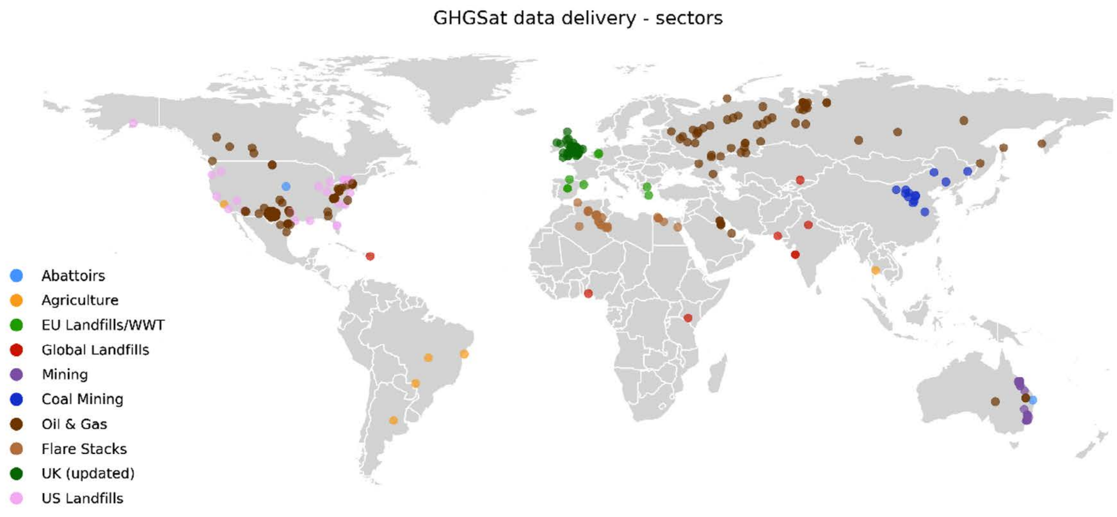

Figure 3-5: *Distribution of GHGSat data locations and associated industry sectors.*

(Figures 3-6) and *(3-7)* describe the number of satellite observations and identified emission plumes at each location - described by the radius of the circle at each site location.

On average, Landfills produced the largest average number of observations per location (6.7), followed by Agriculture (6.5), Mining (3.7), with Oil and Gas producing the fewest (1.9). Agricultural sites produced the highest average number of emission plumes per site (10.4), followed by Mining (8.7). Landfills (8.5), with Oil and Gas again producing the fewest (3.4).

An EU Landfill/Wastewater Treatment (WWT) site in Spain has the largest number of satellite observations (40), and the largest number of individually identified emission plumes (77). Table 1-1 describes, per sector, the sites with the largest number of observations and emissions.

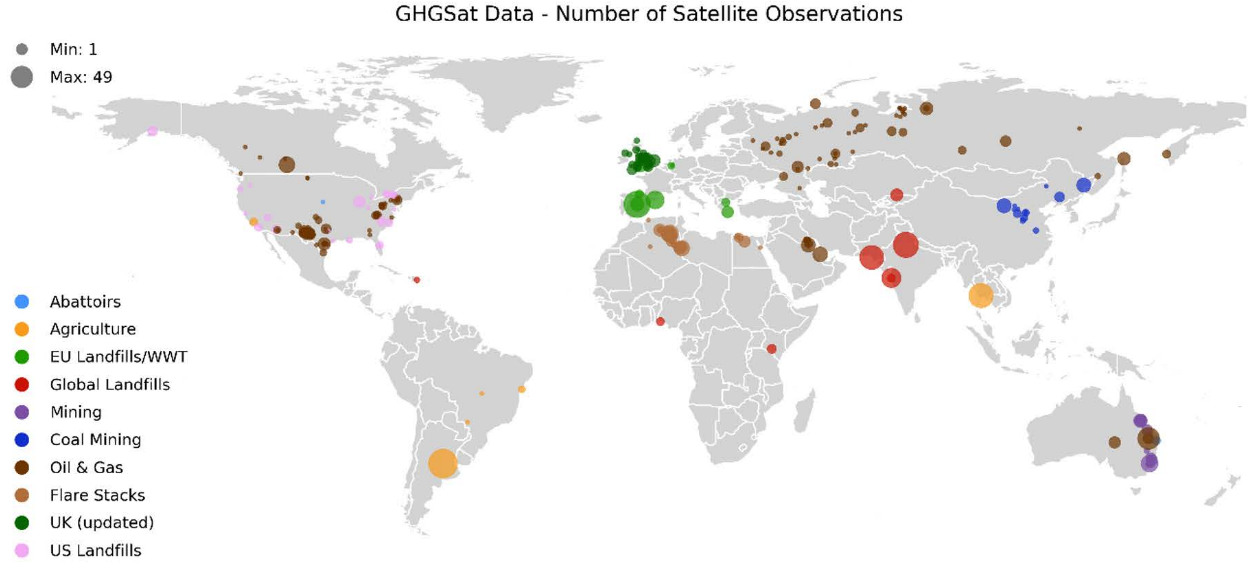

Figure 3-6: *Distribution of GHGSat data locations and associated industry sectors. Number of satellite observations at each location represented by the size of the coloured circle.*

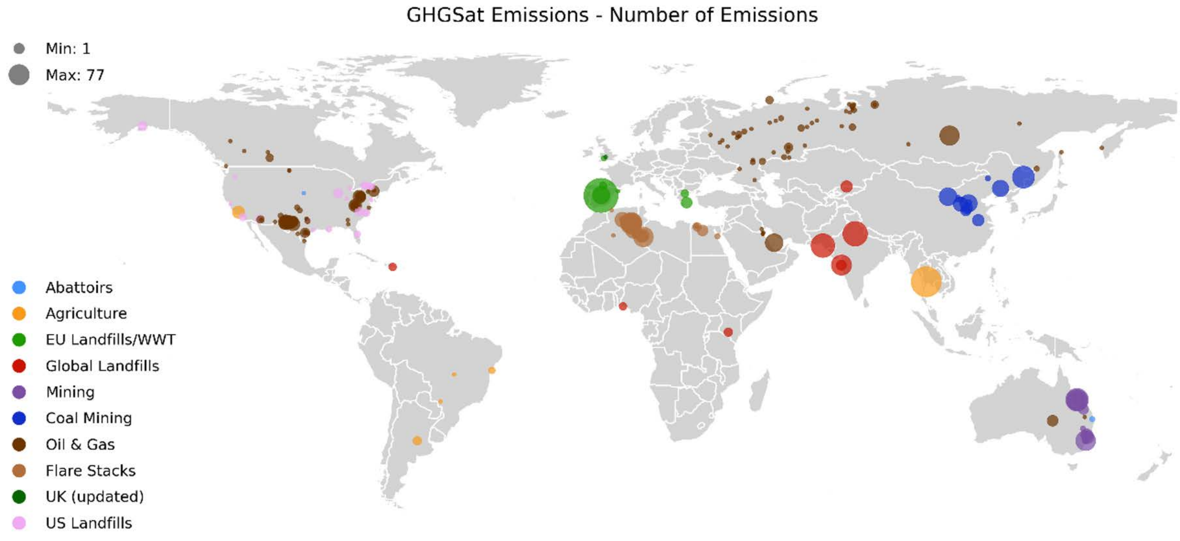

Figure 3-7: *Distribution of GHGSat data locations and associated industry sectors. Number of emission plumes identified defined by the size of the coloured circle.*

Table 1-1: Site locations which provide the largest number of satellite observations and identified emissions plumes.

Sector	Country	Lat	Lon	No of Observations	No of Emissions	Greatest number of
EU Landfills / WWT	Spain	40.26	-3.64	40	77	Emissions and Observations
Oil and Gas	Qatar	25.903	51.508	13	-	Observations
	Russia	58.43	107.37	-	25	Emissions
Global Landfills	India	28.624	77.327	38	40	Emissions and Observations
Agriculture	Thailand	14.06	99.96	35	60	Emissions and Observations
Coal Mining	China	45.8	130.91	12	32	Emissions and Observations
US Landfills	USA	61.291	-149.604	6	6	Emissions and Observations
Abattoirs	Australia	-27.613	152.834	2	2	Emissions and Observations
Mining	Australia	-34.181	150.72	17	-	Observations
	Australia	-21.753	147.991	-	34	Emissions
Flare Stacks	Algeria	31.86	6.174	18	-	Observations
	Algeria	31.8	5.97	-	31	Emissions

The temporal frequency of data (observations and emission plumes) availability is shown in *(Figure 3-8)*. This shows the sites grouped into the four main sector groups (Landfills, Oil and Gas, Agriculture, and Mining), with Oil and Gas maintaining the largest availability of data since January 2021 *(Figure 3-8)(a)*. No Agricultural data is available prior to November 2021.

In each sector, the number of data increases from May 2022 (following the increased number of satellites). Following May 2022, Oil and Gas sites show a notable peak in the number of satellite observations *(Figure 3)*(b) during August 2022 (35), January 2023 (42), while the number of emissions identified increases during July 2022 (53), September 2022 (65), and January 2023 (72). The Mining sector sees a smaller peak in observations during August 2022 (14), with a simultaneous peak in emission (38). Landfills do not observe an immediate increase in data following the May 2022 constellation additions, with initial peaks in observations occurring between January and April 2022 (average of 11), followed by peaks in July 2022 (12), November 2022 (17) and February 2023 (25). Landfill emissions follow the same trend as observations, with a maximum number of emissions in February 2023 (32). Agricultural sites present no obvious spikes in observation frequency, with the number of observations and emissions increasing steadily from September 2022, with a peak of 11 observations and 18 emissions in March 2023.

(a)

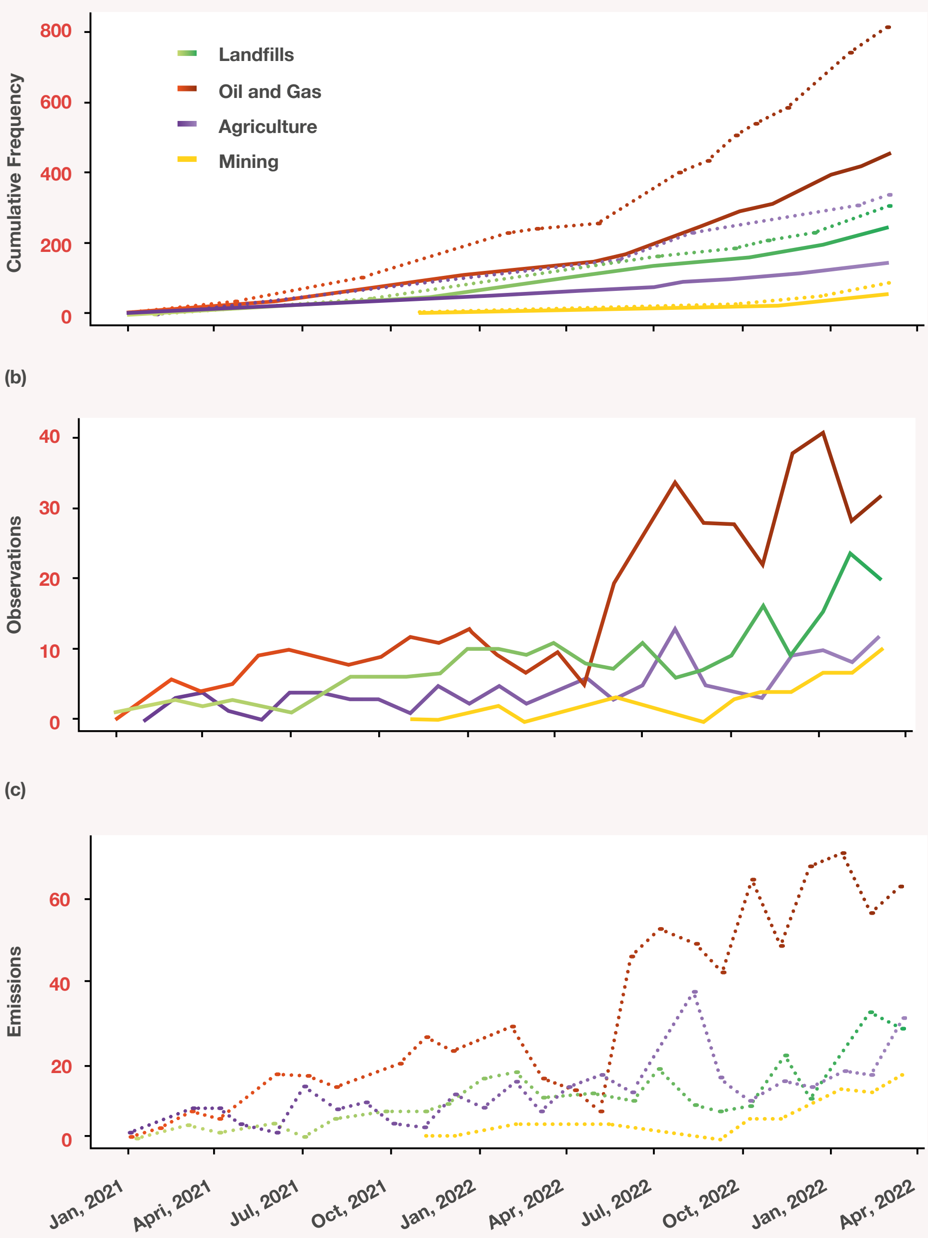

Figure 3-8: Cumulative time series of GHGSat observations (dashed line) and emission plumes (solid line) by industry sector.

Emission flow rate data

For each emission plume identified, a methane emission source rate (kg/h) is calculated. The typical emission characteristics are described by the median flow rate per sector *(Figure 3-9)* and Table 2-1. The 25th and 75th percentile statistically describe the distribution of values within each sector, while the standard deviation (SD) describes the amount variance (about the mean) in emission values per sector.

EU Landfills and Wastewater Treatment (WWT) facilities measured the highest median of 3615 kg/h (4th largest average 3770 kg/h), with a standard deviation (SD) of 1789 kg/h and a maximum emission rate of 6674 kg/h. By comparison, landfills from around the world (Global Landfills) observed similar median and mean emission rates (2,619.5 and 3,780.9kg/h respectively), but produced larger variance, with greater emissions from sites in India compared to those in Africa and the West Indies. US Landfills observed comparatively low emission rates, with median and mean emission values less than half of those from the EU (median = 1,207 kg/h / mean = 1,514 kg/h).

Coal mining in China observed the second largest median emission flow rate (3051 kg/h) and the largest average rate (5489 kg/h), producing the largest variance in emission rates (SD = 7019 kg/h), with several locations generating the majority of large emissions *(Figure 3-10* and *3-11)*, including a maximum rate of 38,478 kg/h. Mining locations in Australia produced similar emission statistics to those in China, with a median and mean emission rates of 2,942 and 3,932 kg/h respectively, with the largest single emission measurement of 39,614 kg/h but a comparatively small SD of 3,444.8 kg/h.

Oil and Gas fields and Flare Stacks produced some of the lowest median and average emission rates of all sectors (>2,000 kg/h) with the oil fields showing greater variance (2,013 kg/h) compared to the Flare Stacks (1,214 kg/h).

The six Agriculture locations observed the lowest median (1,072 kg/h) and mean (1,260 kg/h) emission rates of all the industrial sectors, with a maximum of 5,327 kg/h.

The two Abattoir sites produced a mean and median (2,471 kg/h) emission rates moderately less than landfill and coal mining sites, with a maximum of 4,251 kg/h.

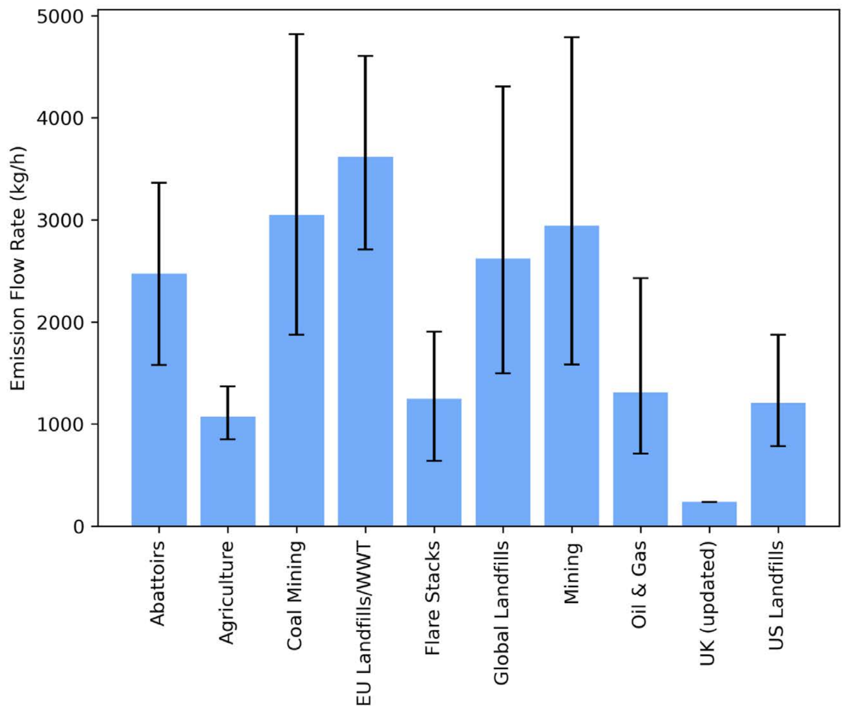

Figure 3-9: Median methane emission flow rate (kg/h) per sector. Bars represent distribution of methane emission values by the 25th and 75th percentile.

Table 1-2: Descriptive statistics of methane emission flow rate (kg/h) per industry sector as measured by GHGSat WAF-P sensors between November 2020 - March 2023.

	Mean	Median	SD	Max	Count
Abattoirs	2,471.0	2,471	2,517.3	4,251	2
Agriculture	1,260.2	1,072.5	763.2	5,327	6
Coal Mining	5,489.3	3,051	7,019.6	38,478	13
EU Landfills/WWT	3,770.1	3,615	1,789.9	17,873	7
Flare Stacks	1,494.6	1,248	1,213.8	5,973	27
Global Landfills	3,780.9	2,619.5	3,572.1	15,030	8
Mining	3,932.5	2,942	3,444.8	39,614	25
Oil and gas	1,999.9	1,312	2,013.4	20,623	215
UK (updated)	236.0	236	-	236	1
US Landfills	1,514.1	1,207	917.1	4,330	21

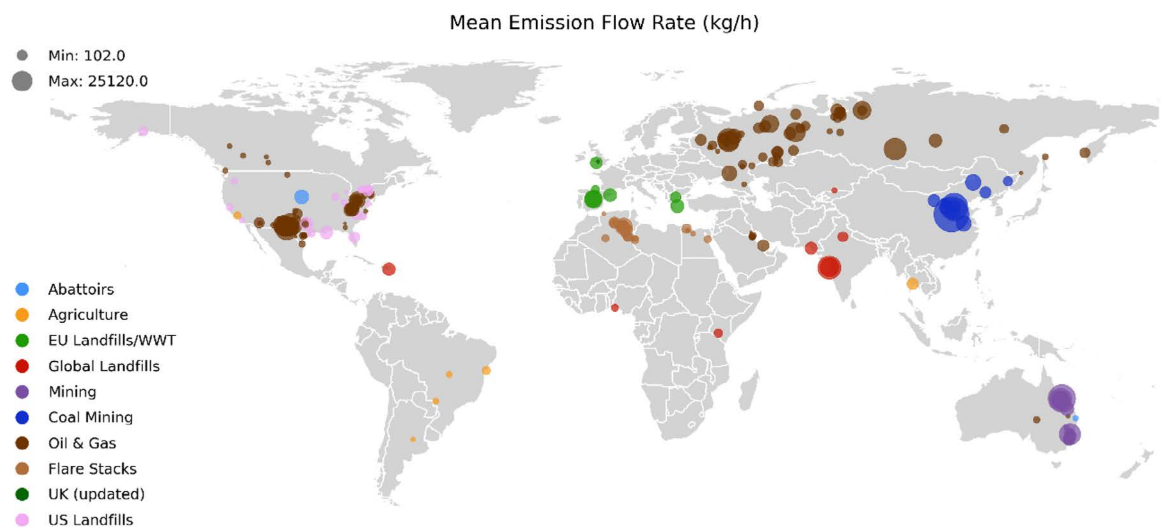

Figure 3-10: *Mean methane emission flow rate (kg/h) observed by GHGSat satellites at individual site locations between November 2020 – March 2023.*

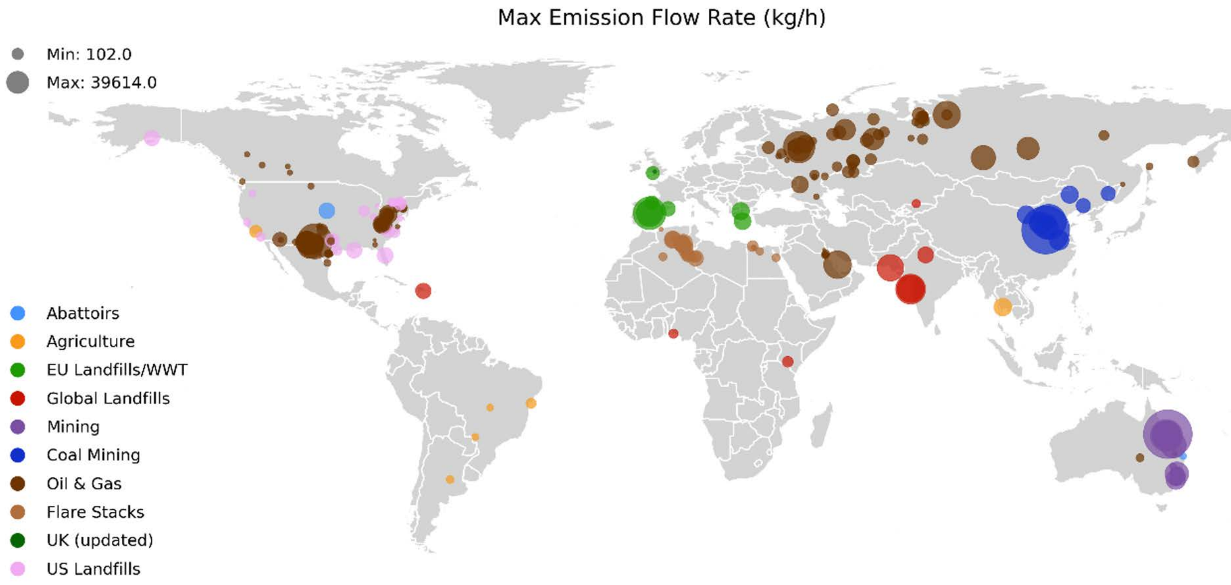

Figure 3-11: *Maximum methane emission flow rate (kg/h) observed by GHGSat satellites at individual site locations between November 2020 – March 2023.*

Abundance data

The 443 Abundance Data Products cover 161 different locations, including 6 different industries and all UK satellite observations *(Figure 3-12)*. Oil and Gas sites cover 62% (100) of the locations, providing 52% (230) of all observations. UK sites produce the second largest number of locations (41), providing 25.5% of all locations, and 25.8% of all observations. EU and US landfills cover abundance data twelve sites (7.5%), providing 9.9% (44) observations. A total of six mining locations provides nine Abundance Data Products. Abattoirs and agriculture sites each provide one abundance data site, providing two and forty-four observations respectively.

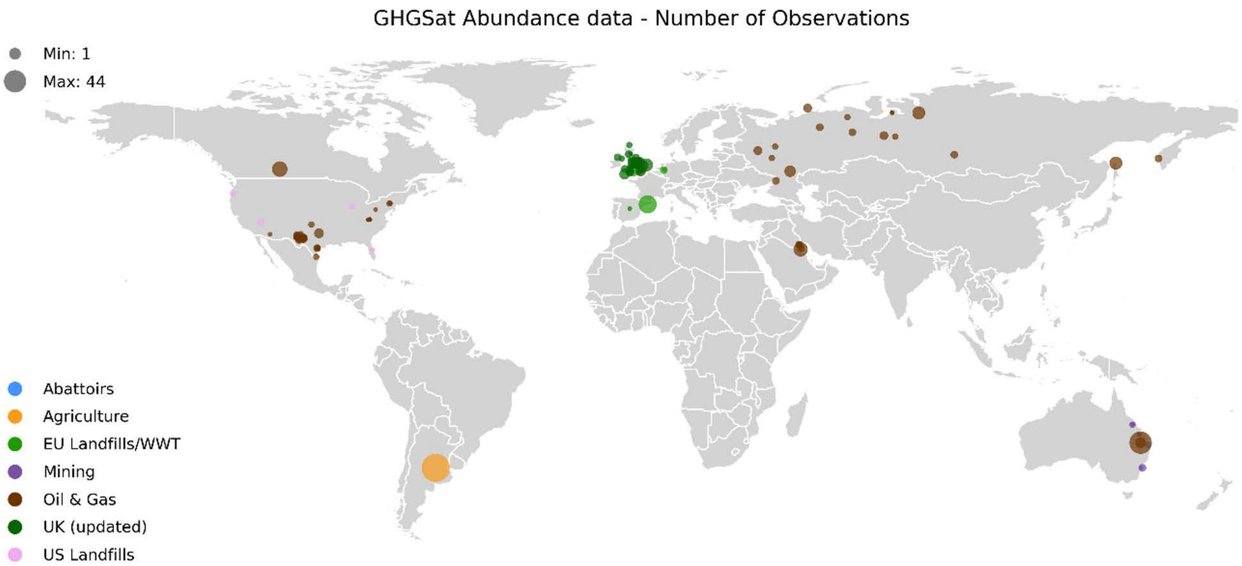

Figure 3-12: *Distribution of GHGSat data locations and associated industry sectors. Number of null abundance observations made at each location defined by the size of the coloured circle.*

UK data

As part of the data acquisition project, all GHGSat data for the UK will be made available to eligible users. The initial data delivery includes 123 satellite observations, covering the period from November 2020 to March 2023. The UK dataset includes only three observed emissions from two locations, with all other observations providing null Abundance Products (no emission observed) *(Figure 3-13)(a)*.

Currently, UK observations cover 42 individual sites *(Figure 3-13)(a),* including facilities from four key industrial sectors: Power Stations (Power Generation), Waste Management, Mining, and Oil & Gas extraction and processing *(Figure 3-13(b)*.

The number of satellite observations vary per location *(Figure 3-13)* and industry sectors *(Figure 3-14).* From the 42 locations, Water Waste Management contributes the largest number with 18 sites (43%), followed by Mining (14 sites / 33%), Oil and Gas (9 / 21.4%), with only one Power Station location. From these sites, Waste Management have the largest number of satellite observations with 51 (42.9%), followed by Mining (35 / 27.8%), Oil and Gas (26 / 20.6%), with the one power station producing 11 observations, which is the largest number of observations of any single location *(Figure 3-13(b)*.

Observations occur only during cloud-free conditions, with the frequency of successful (cloud free) observations varying throughout the time series *(Figure 3-15)*. The largest number of observations occurred in January 2023 (14), while July 2022 saw the largest number of observed emissions (2).

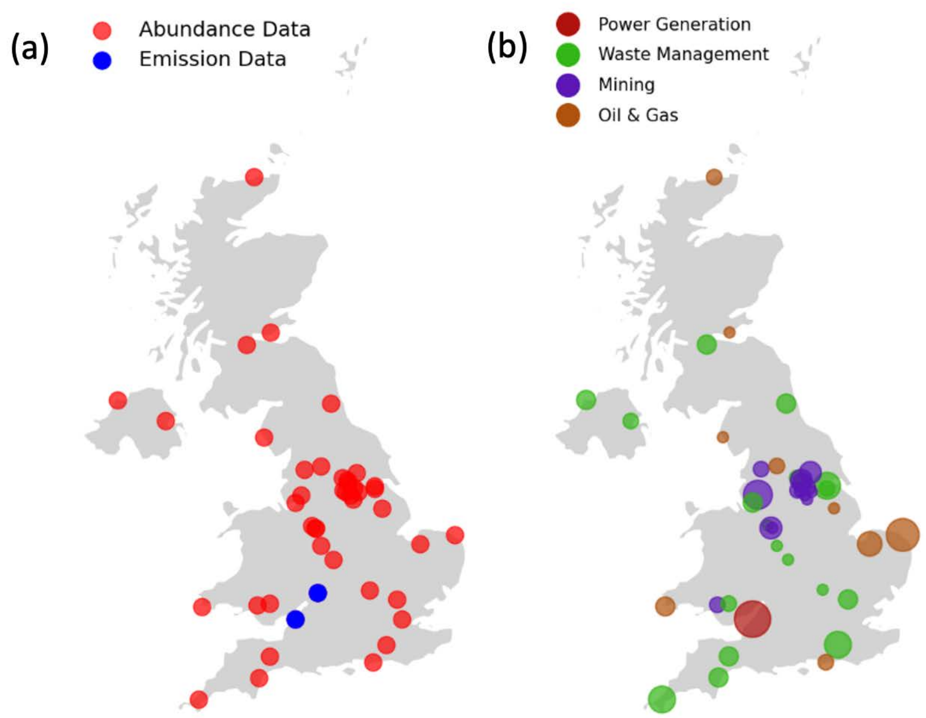

Figure 3-13: *Distribution of GHGSat data for the UK, including a) location of emission and abundance (null) data, and b) number of satellite observations (radius of circle, Min = 1, Max = 11) and industry sector.*

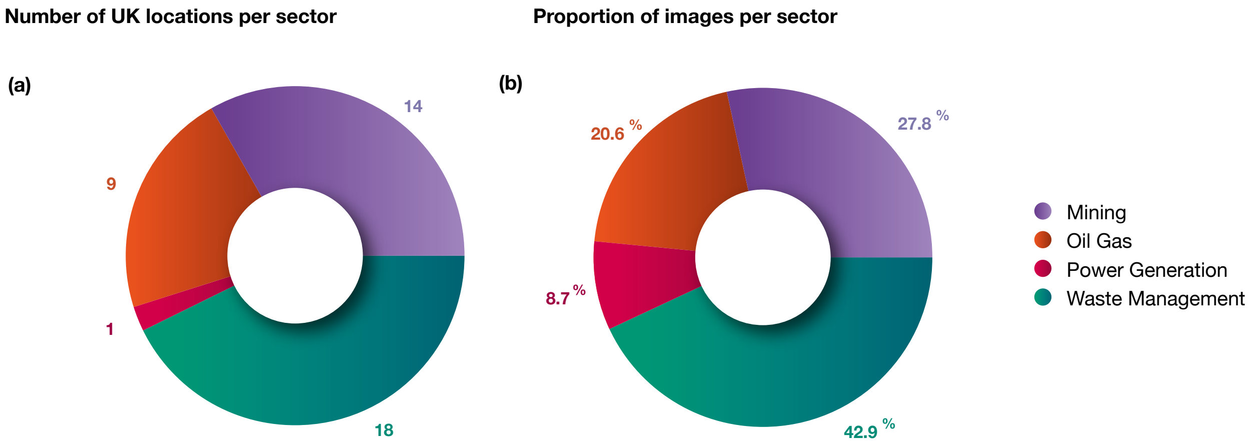

Figure 3-14: GHGSat UK data distribution by industry sector, showing number of a) locations and (b) satellite observations.

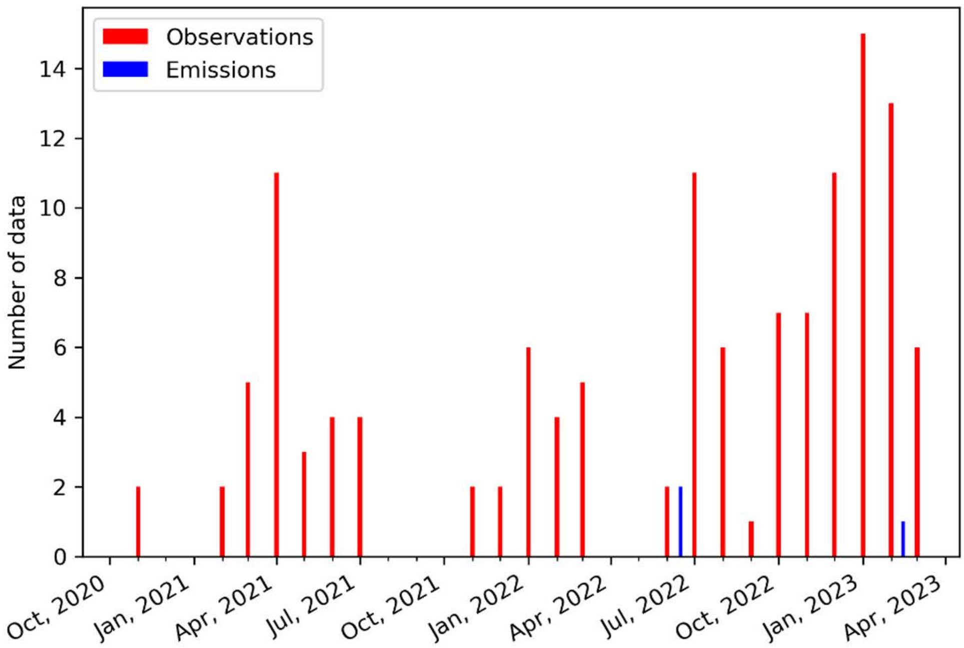

Figure 3-15: Time series of GHGSat emission and abundance data for the UK.

4. Accessing the SPECTRA data portal

Following an initial consultation with either SAC, OS, or DEFRA, you will have been set up as a premium user to gain access to GHGSat's online data portal SPECTRA.

You will receive an email inviting you to complete your user set-up, where you will need to create a login password.

You can now access the SPECTRA portal by either visiting https://spectra.ghgsat.com/account/login or through the GHGSat website - where you should navigate to the menu in the top right of the screen, and select Log In to your Premium Account *(Figure 4-1)*.

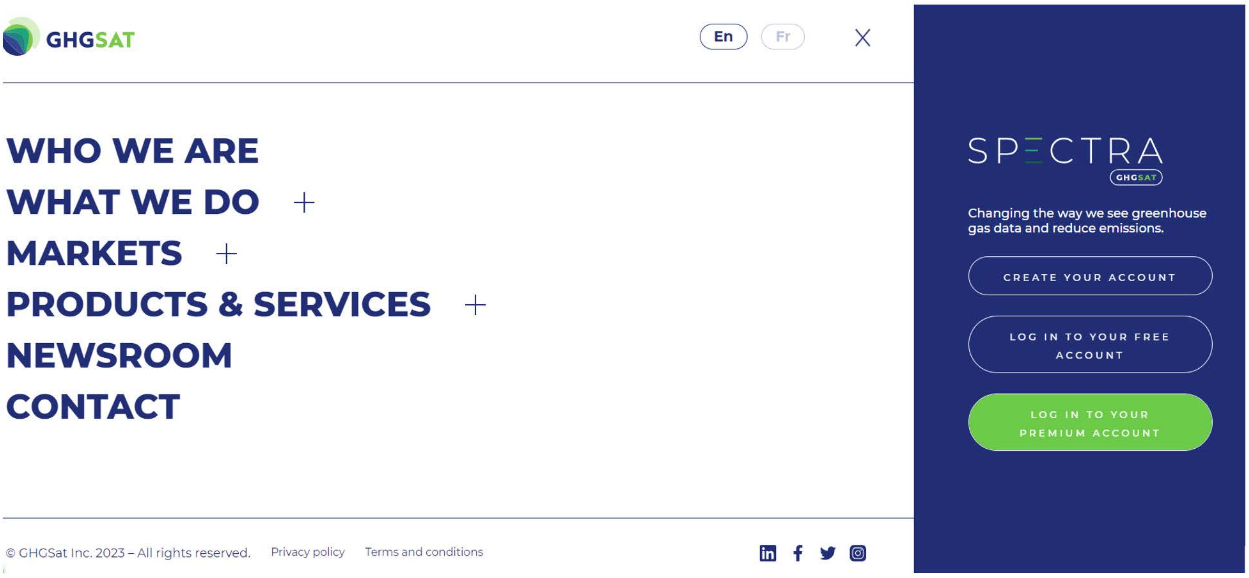

Figure 4-1: *GHGSat website, select 'Log In to your Premium Account' to enter the Spectra Portal with your user login details (Figure 4-2).*

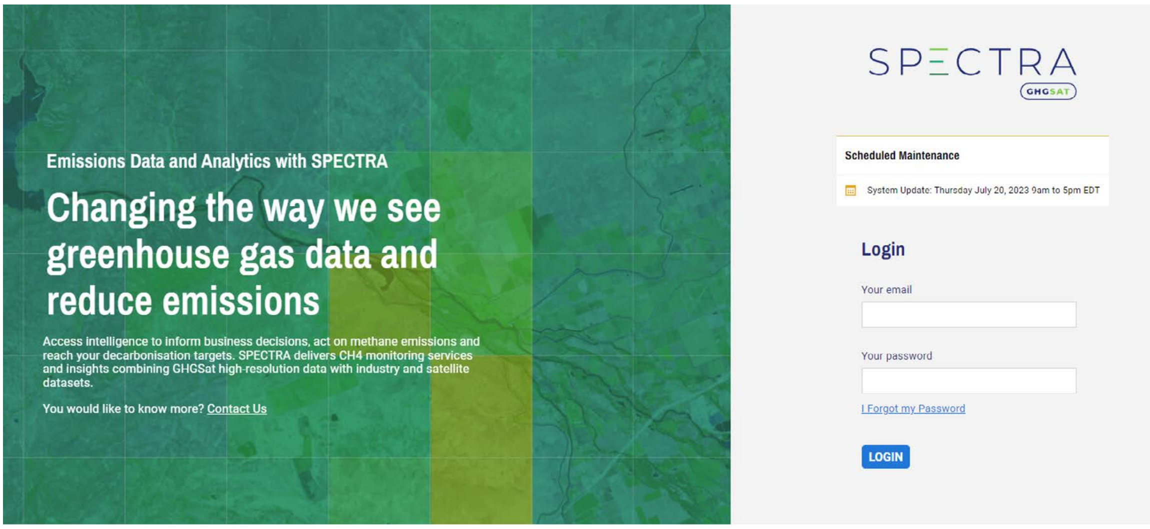

Figure 4-2: *Login page for GHGSat SPECTRA data and analytics portal: Login at Spectra*

5. SPECTRA user interface overview

The SPECTRA data portal provides data search and visualisation options for GHGSat data. Through this portal, users can access the data provided via the UKSA project. The SPECTRA interface has two principal user view options, the [Map View](#), and [List View](#). Users can toggle between Map and List view by selecting the relevant tab in the SPECTRA window (object 1 in *Figure 5-1*). Guides on how to use these views are provided in the following sections.

Map View

The Map View is your default SPECTRA window, where you can visualise GHGSat data in a geographical context *(Figure 5-1)*. Similar to many GIS applications, the Map View allows the user to select different layers of data to aid visualisation. The Map View contains useful tools, which allow the user to search, sort and visualise the data (Table 5-1).

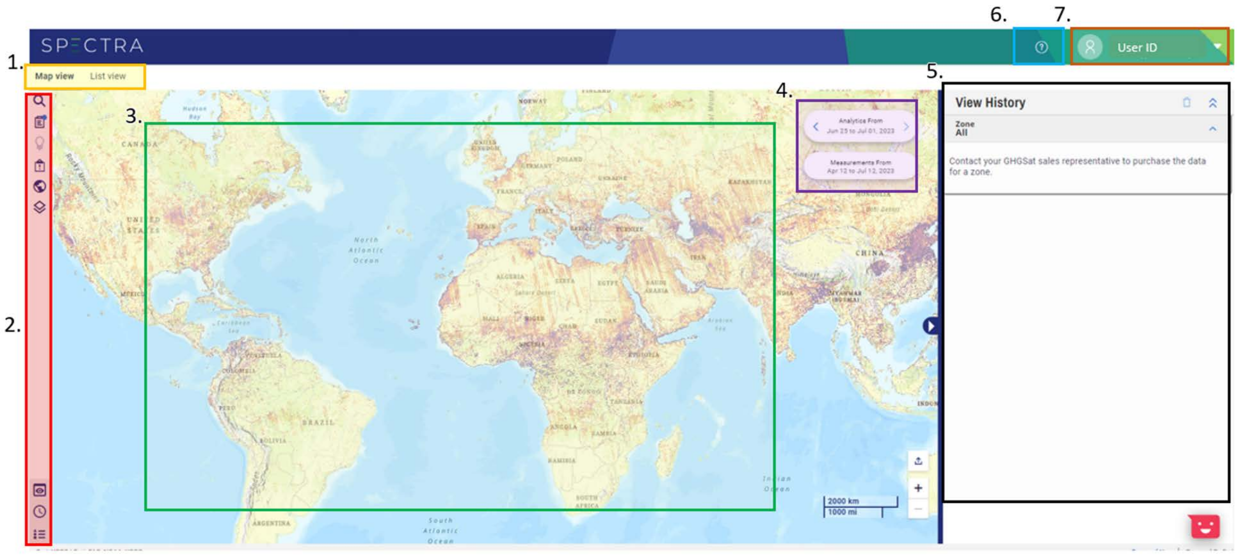

Figure 5-1: *Map View display in SPECTRA data portal. Key tools and features are highlighted and numbered, with description provided in Table 5-1.*

Table 5-1: Key features and tools available in Map View in the SPECTRA data portal. Numbers relate to highlighted areas in Figure 5-1. Source: GHGSat

1	**Toggle between Map View and List View**	Map View: Visualise data products in a geographical context, with key information displayed in the View History information panel (object 5)
		List View: View and sort available data products by multiple attributes (see section (List View data search for more information)
2	**Map View data search and visualisation tools**	Search for a location or a site
		Display latest news from GHGSat
		View the largest emitting sites or those that are at risk for an emission
		View notifications when emission detected at tasked location
		Choose a basemap
		Show or hide different dataset layers
		Create a saved display
		View data according to specific timeline
		View the Map Legend
3	**Data Visualisation window**	View emission plumes in a GIS environment
		Display data with a number of complimentary data layers, available from the Data Layers tool
		By default, Sentinel-5 TROPOMI average concentration data are displayed as a base layer. These data are aggregated for the period defined in the Analytics date range (object 4)
4	**Analytics Date Range selection**	Define the period of time to aggregate background methane concentration data in the main data visualisation window (object 3)
5	**View the History and product information window**	Display data analytics from observed plume rasters
		Dynamic display that will change depending on which data is selected
6	**Help button**	Access to SPECTRA portal help, including API instructions, User management, FAQs, and Glossary
7	**Profile management**	Manage user account information, Bookmark certain data views, receive reports on tasked locations, and amend settings

List View

Available GHGSat data sets are displayed in the List View display. Here data can be viewed in one of three tabs, including:

Site Location tab

- Currently, no data are available in the Site Locations tab

Observation List

- Data are described by the observation ID, which represents the unique identifier for a single satellite observation 12 km^2 footprint *(Figure 5-2)*
- These data describe both Abundance and Emission data
- Data are attributed with key metadata, including observation date and time, corresponding satellite (C1 to C8) and geographical zone
- Availability of emission plume within the footprint are described as Yes or No (Y/N)
- Where emission plumes are identified, the sum of all emissions rates observed are presented

Emission List

- Data are described by a unique emission plume ID *(Figure 5-3)*
- Each plume is attributed with multiple metadata, including decimal degrees geographical coordinates of the source location (Latitude and Longitude), observation date and time, corresponding satellite (C1 to C8), and geographical zone and site name (if available)
- Emission rate is presented, and an error rate analysis is given as a percentage
- A list of available data is available as a .csv download using the Download List View button. This list can be filtered, using the filter icon ( ) – see Data Search: List View

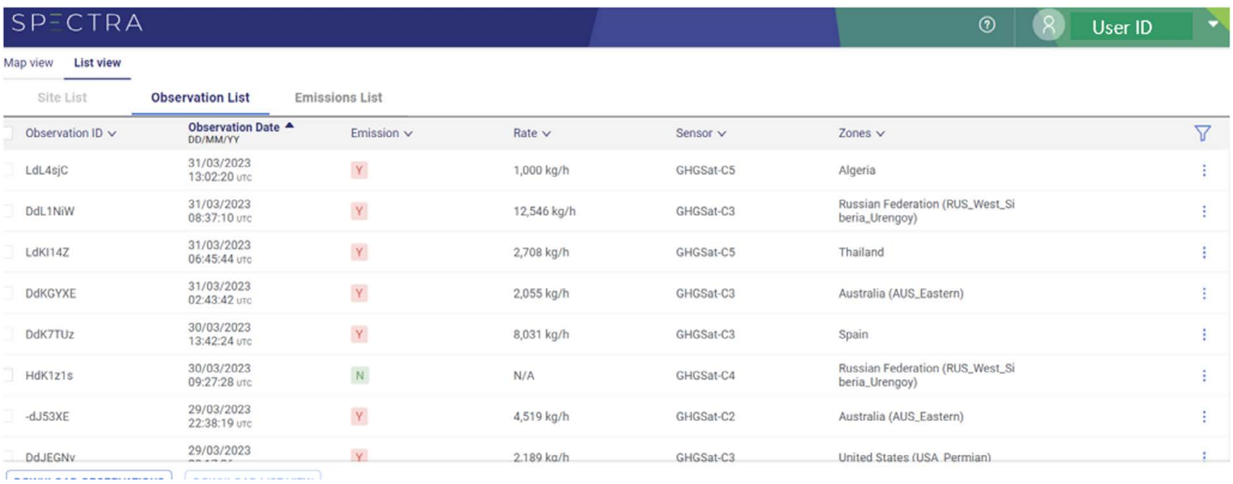

Figure 5-2: *List View displaying both available abundance and emission data. Each observation is attributed with multiple information, which is searchable through the filter tool. Source: GHGSat*

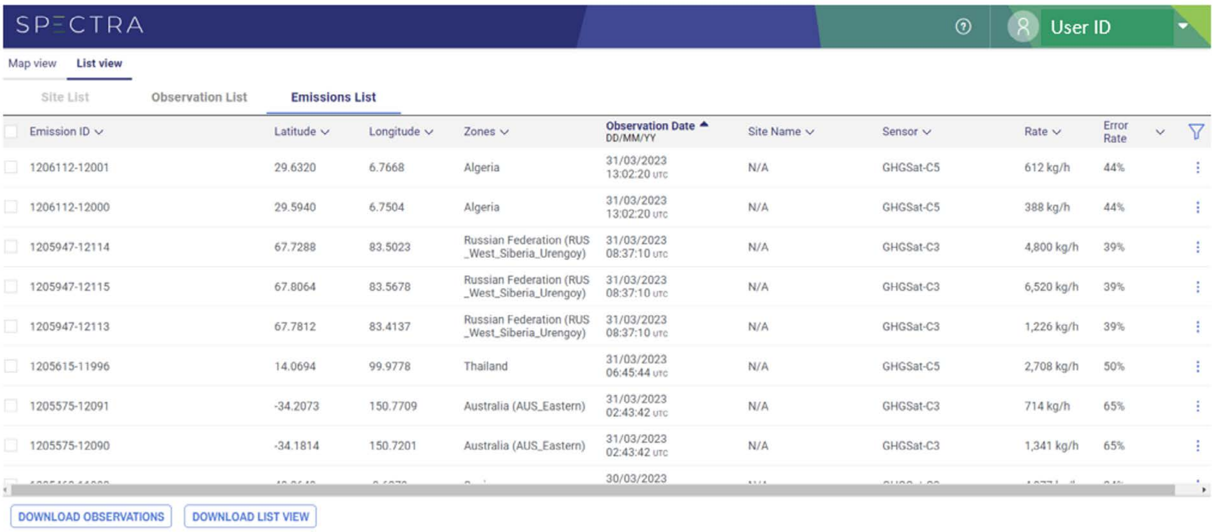

Emission ID	Latitude	Longitude	Zones	Observation Date DD/MM/YY	Site Name	Sensor	Rate	Error Rate
1206112-12001	29.6320	6.7668	Algeria	31/03/2023 13:02:20 UTC	N/A	GHGSat-C5	612 kg/h	44%
1206112-12000	29.5940	6.7504	Algeria	31/03/2023 13:02:20 UTC	N/A	GHGSat-C5	388 kg/h	44%
1205947-12114	67.7288	83.5023	Russian Federation (RUS _West_Siberia_Urengoy)	31/03/2023 08:37:10 UTC	N/A	GHGSat-C3	4,800 kg/h	39%
1205947-12115	67.8064	83.5678	Russian Federation (RUS _West_Siberia_Urengoy)	31/03/2023 08:37:10 UTC	N/A	GHGSat-C3	6,520 kg/h	39%
1205947-12113	67.7812	83.4137	Russian Federation (RUS _West_Siberia_Urengoy)	31/03/2023 08:37:10 UTC	N/A	GHGSat-C3	1,226 kg/h	39%
1205615-11996	14.0694	99.9778	Thailand	31/03/2023 06:45:44 UTC	N/A	GHGSat-C5	2,708 kg/h	50%
1205575-12091	-34.2073	150.7709	Australia (AUS_Eastern)	31/03/2023 02:43:42 UTC	N/A	GHGSat-C3	714 kg/h	65%
1205575-12090	-34.1814	150.7201	Australia (AUS_Eastern)	31/03/2023 02:43:42 UTC	N/A	GHGSat-C3	1,341 kg/h	65%

Figure 5-3: *List View displaying available emission data only. Each emission plume data is attributed with multiple information, which is searchable through the filter tool. Source: GHGSat*

6. Data Search and Discovery

As part of this initiative, users have access to both Abundance *(Figure 2-2(c)* and Emission *(Figure 2-2(d)* Datasets. Using SPECTRA's search options, users can identify which data is available within their region and time of interest. This can be done in either the Map or List view tabs, as described below.

The search option you choose will depend on your type of search.

- If you are looking for a specific location, then the Map View tab will be more efficient, as it allows you to focus your search by area
- If you are looking to search all data by geographic region (e.g., country), or emission rate, then sorting through the data on the List View tab will be the best option

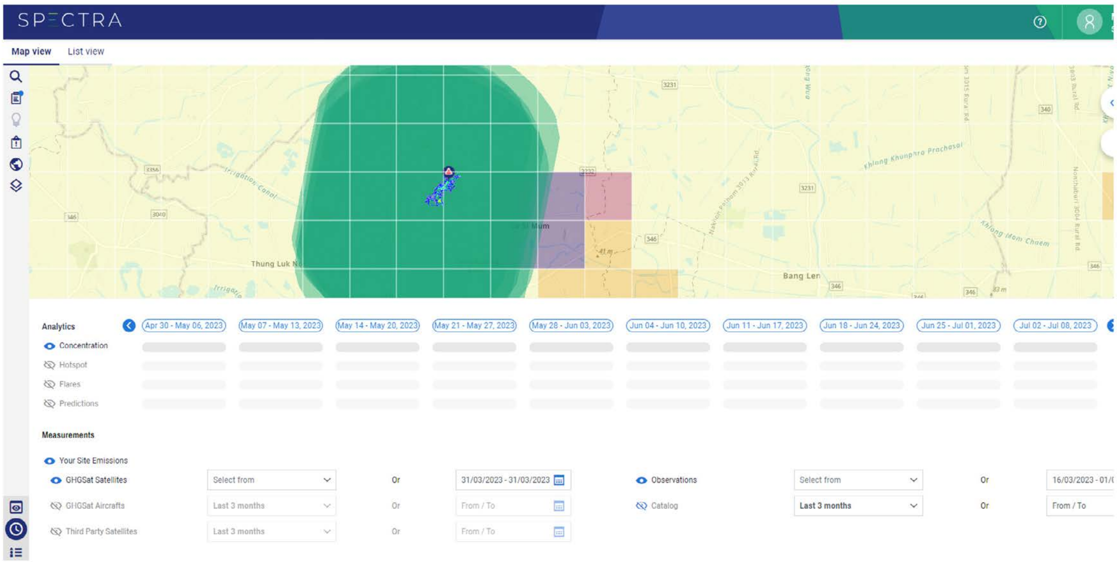

Figure 6-1: *Map View timelines search option. Map Display shows available observation footprint (green area) and identified emission plume (source indicated by red triangle). Background gridded data describes mean methane concentrations from TROPOMI (Sentinel-5p) data for the period July 09-July 15, 2023. Source: GHGSat*

Data Search: Map View

- Using either your mouse or the search tool (on the left side toolbar), zoom into your geographical area of interest
- Select the timelines icon (on the left side toolbar) to define the time period of interest *(Figure 6-2)*
- The timelines panel is divided into two sections, Analytics and Measurements
- The Analytics timeline defines the period used to aggregate the background methane concentrations (using TROPOMI data from Sentinel-5). These data are displayed in the main panel as the background raster (orange to red hues in *Figure 6-1*)
- Analytics can be selected for a single week, or an extended period, these data can be displayed as a single image or as a week-by-week animation

- Hotspots, Flares and Predictions data are currently not available in this dataset
- The Measurements timeline defines the search period for available Emissions and Abundance data (described as Observations)
- For either Emissions or Abundance/Observations data, users can search over an extended period (e.g., last 3 months) from the dropdown menu or a specific period using the date select tool
- Any available data within that period will be displayed in the map panel
- The source location of detected methane emissions will be denoted by a red triangle symbol, while abundance data will appear as a green footprint *(e.g., Figure 6-1)*.
- Either emission locations (red triangle) or abundance footprint (green area) data can be selected, producing more information about each data type in the Product History and Information pop-out panel *(Figure 6-2)*

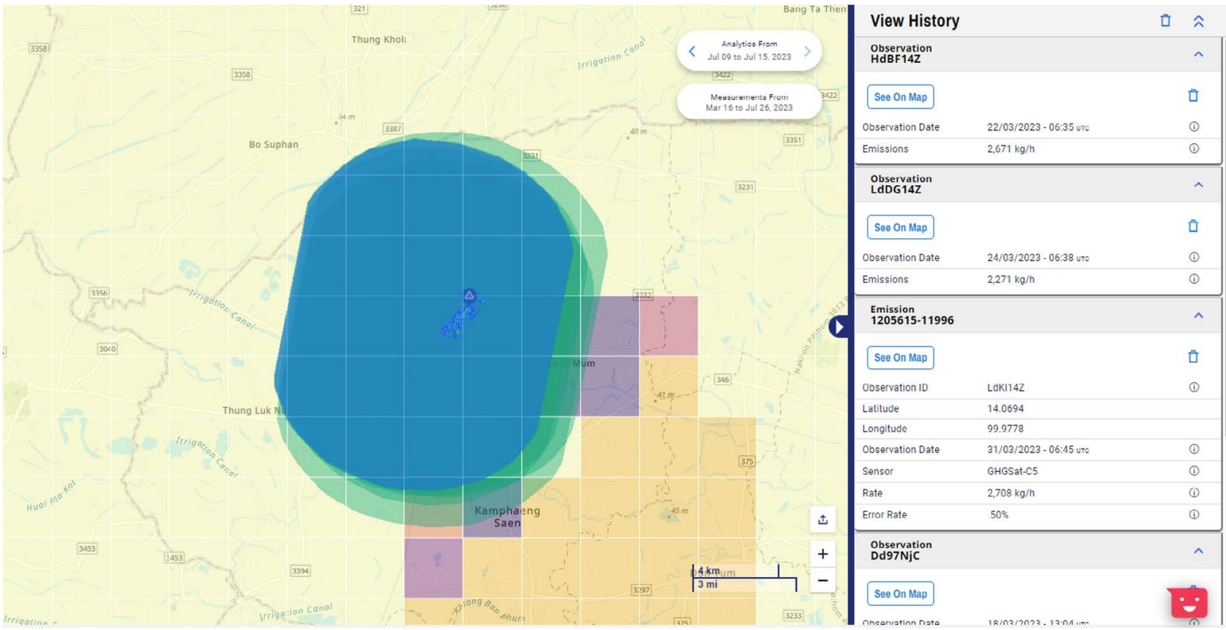

***Figure 6-2:** Product History and Information panel in Spectra Map View. Background gridded data describes mean methane concentrations from TROPOMI (Sentinel-5p) data (July 09-July 15, 2023). Source: GHGSat*

Additional features

- Users can choose to visualise either the emission or observation datasets by toggling the eye symbol / within the Measurements selection or the data layers panel
- With the timeline selected, users can continue to search around the map with their cursor Any data which is available during that period will appear as it comes into the viewer's field of view
- Other Data: When the map is zoomed into an appropriate scale, the Catalogue Visualisation symbol will become available. Users can toggle this on to visualise observations within the field of view and selected observation periods which are not currently available in this dataset but have been observed by GHGSat

- These observations may or may not have emissions observed in them
- Users are recommended to contact either their distributing project partner (SAC/OD/Defra) or GHGSat to enquire about collecting these data
- GHGSat Aircraft Data and Third-Party Satellite Data are not currently available through this SPECTRA account

Data Search: List View

- Using the filter icon, users can subset the available dataset by a number of attribute criteria in either the Observation List tab or Emission List tab

Filter types

- Filters include both Name and Value filters
- Value filters include Emission Rate, Error Rate, and Observation Date, where the user can specify a range of potential values to search the dataset. All other fields require matching attribute information, such as Zone (country), Observation/Emission ID
- Filter options are live, meaning the user does not need to fill in the entire field before the list filters. Using this option, users can effectively search the data without knowing the full information
- This can be useful when the user only knowing the exact zonal information, or Emission/Observation ID

Multiple filters

- Users can apply multiple filters to narrow search results
- Example User Request:
    - All emission plume data
    - Location: Permian Basin (USA)
    - Period: October to December 2022
    - Emission Rate: >500 kg/hr
    - Error Rate: <40%

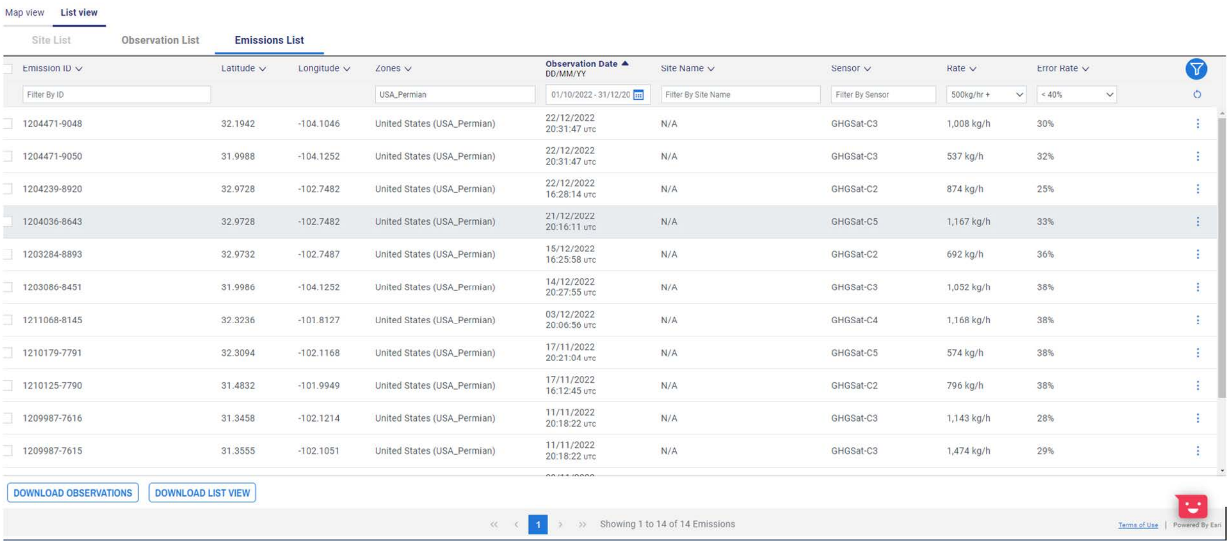

Map view List view

Site List Observation List Emissions List

Emission ID	Latitude	Longitude	Zones	Observation Date DD/MM/YY	Site Name	Sensor	Rate	Error Rate
Filter By ID			USA_Permian	01/10/2022 - 31/12/20	Filter By Site Name	Filter By Sensor	500kg/hr +	< 40%
1204471-9048	32.1942	-104.1046	United States (USA_Permian)	22/12/2022 20:31:47 UTC	N/A	GHGSat-C3	1,008 kg/h	30%
1204471-9050	31.9988	-104.1252	United States (USA_Permian)	22/12/2022 20:31:47 UTC	N/A	GHGSat-C3	537 kg/h	32%
1204239-8920	32.9728	-102.7482	United States (USA_Permian)	22/12/2022 16:28:14 UTC	N/A	GHGSat-C2	874 kg/h	25%
1204036-8643	32.9728	-102.7482	United States (USA_Permian)	21/12/2022 20:16:11 UTC	N/A	GHGSat-C5	1,167 kg/h	33%
1203284-8893	32.9732	-102.7487	United States (USA_Permian)	15/12/2022 16:25:58 UTC	N/A	GHGSat-C2	692 kg/h	36%
1203086-8451	31.9986	-104.1252	United States (USA_Permian)	14/12/2022 20:27:55 UTC	N/A	GHGSat-C3	1,052 kg/h	38%
1211068-8145	32.3236	-101.8127	United States (USA_Permian)	03/12/2022 20:06:56 UTC	N/A	GHGSat-C4	1,168 kg/h	38%
1210179-7791	32.3094	-102.1168	United States (USA_Permian)	17/11/2022 20:21:04 UTC	N/A	GHGSat-C5	574 kg/h	38%
1210125-7790	31.4832	-101.9949	United States (USA_Permian)	17/11/2022 16:12:45 UTC	N/A	GHGSat-C2	796 kg/h	38%
1209987-7616	31.3458	-102.1214	United States (USA_Permian)	11/11/2022 20:18:22 UTC	N/A	GHGSat-C3	1,143 kg/h	28%
1209987-7615	31.3555	-102.1051	United States (USA_Permian)	11/11/2022 20:18:22 UTC	N/A	GHGSat-C3	1,474 kg/h	29%

DOWNLOAD OBSERVATIONS DOWNLOAD LIST VIEW

Showing 1 to 14 of 14 Emissions

Terms of Use | Powered By Esri

Figure 6-3 *Spectra List View description of Emission products available using a filter of Zone (geographical), Date Range, Emission Rate, and Error Rate. Source: GHGSat*

- By entering each of these criteria in the Emissions List Filter tool, the user will discover 14 emissions *(Figure 6-3)*
- The filtered list can be sorted alphabetically or by value in an ascending or descending order by toggling the direction arrow next to the column heading
- The filtered data can be downloaded as either a list (.csv spreadsheet), or as a .zip file of individual concentration maps

Viewing the required emissions in Map View

  - First, select the check box to the left of each emission row that needs to be visualised
  - With each emission selected, click the three dots to right on one of the emission rows (this will be the emission you will be directed to)
  - Selecting See On Map, the user will be redirected to the Map View where the emission plume will be presented in a geographical context (See Visualise Data for more options)
- Alternatively, users can use the View Emission option to see a concentration map, where the emission plume is presented (in a new window) over high-resolution satellite imagery of the surrounding surface (provided by Mapbox)

7. Data Viewing and Visualization

SPECTRA offers the users the opportunity to visualise the extent any of the available emission plume data within the Map View screen.

Which emission plumes will be visualised? This is defined by the user's data search parameters, described either within the *Map View Timelines tool* or by selection within the *List View tab*.

Once the emission plume(s) have been selected in the Map View, there are several options to alter how they are visualised on screen.

Basemap

Using the Basemap icon, users can select between Topographic or Satellite Basemap. Topographic maps will give added context to the plume geometry – e.g., clearly describing the geometry of an open-pit mine *(Figure 7-1)*

Satellite maps will provide visual clues to the features at the source of the emission plume, helping to identify which part of a facility is likely to be contributing to the observed plume.

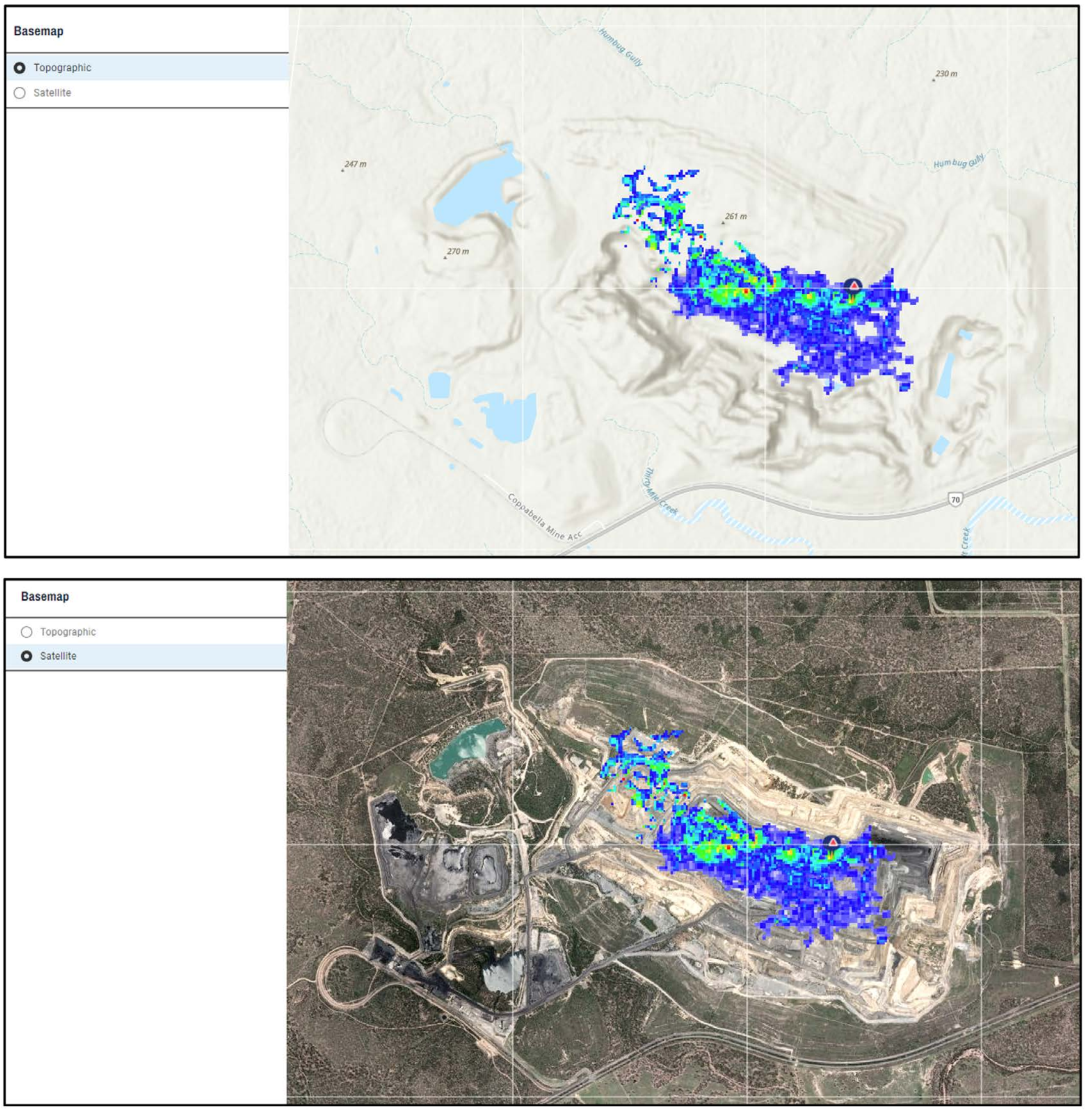

Figure 7-1: *Different Basemap viewing options for emission plume observed near an open-pit mine in Western Australia (-21.85N, 148.49E). Source: GHGSat*

Data Layers

Using the Data Layers tool , users can select which data layers (Table 7-1) are visible in the main screen, by toggling the visibility symbol / next to the relevant layer *(Figure7-2)*.

For this data collection, many of the layer options are not available (appearing grey). Some of the options will only be available at the correct scale/zoom. These are indicated by a ⓘ and include Zone, Observations and Catalogue.

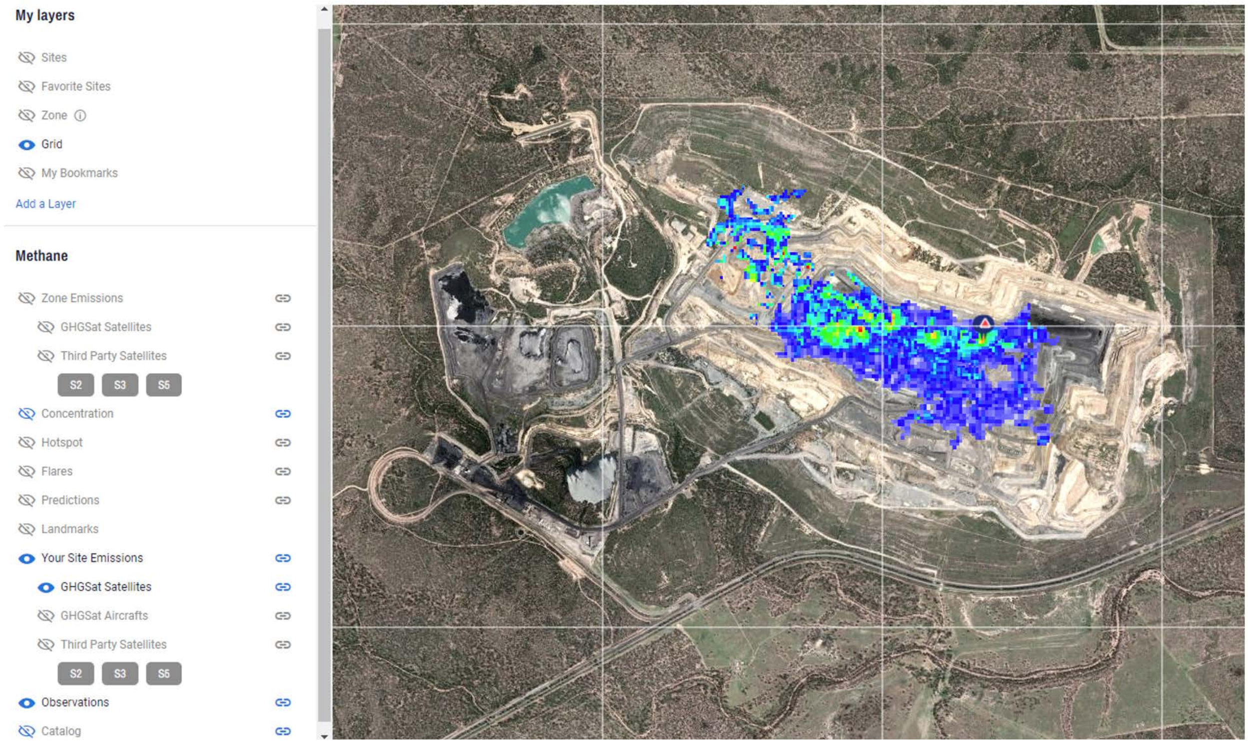

Figure 7-2: *My Layers options in SPECTRA data portal. Main window shows emission plume observed near an open-pit mine in Western Australia (-21.85N, 148.49E). Source: GHGSat*

Table 7-1: Description of each of the layer options when visualising data within the Spectra Map View. Source: GHGSat

Sites	The Sites layer displays site details including site names, coordinates, and the type of facility, such as a compressor or a well pad.	
Favourite Sites	The Favourite Site layer consists of "bookmarked" sites which can be selected and applied as a favourites layer, similar to how websites can be bookmarked as favourites.	
Zone	The Zone layer is a layer of geographical areas on the map (e.g., ESP - Spain). When the Zones layer is selected, the sites and assets contained in the Zone dataset are displayed.	
Grid	A Grid layer is a layer of grids (squares) that can be applied to either the Basemap or Topographic map in Map View.	
My Bookmarks		
Add a Layer	This option is available in the Data Layers panel. It allows you to connect to layers from external GIS software and display them in SPECTRA's Map View.	
Methane		
Zone Emissions	Zone Emissions layer displays an icon indicating which emissions occur within each specific zone, this is shown when data is purchased as an entire zone.	
Concentration	The Concentration layer displays values that estimate how much methane (CH_4) is in the air for each cell in a grid layout. The concentration estimates are measured in parts per billion.	
Hotspot	The Hotspots layer displays values that indicate if the delta is higher than expected between the detected methane concentration and GHGSat's data model for each cell in a grid layout. Hotspot detection may be an indicator of a methane emission or one that is nearby.	
Flares	The Flares layer displays values indicating whether a site device is burning methane.	
Predictions	The Predictions layer displays values that quantify the risk of an emission and the level of certainty or confidence in that risk value for each cell in a grid layout.	
Landmarks		
Your Site Emissions	The Emissions layers display values indicating if an emission is present, measured in kg/hr.	
	GHGSat Satellites	This layer consists of GHGSat satellite emissions observations data.
	GHGSat Aircraft	This layer consists of GHGSat aircraft emissions observations data.
	Third party Satellites	This layer consists of third-party satellite emissions observations data.
Observations	The Observations layer displays a collection of measurements taken by a GHGSat satellite sensor.	
Catalogue	The Catalogue layer displays a library of all observation data collected by GHGSat's satellite sensors.	

My Displays

The My Displays tool, allows the user to save their current viewing options, by selecting the Create New Display button. Once saved, the user will be able to return to the same view, with selected viewing preferences by selecting the relevant My Display save.

Legend

The Legend tool displays the legends for all potential layers (Table 7-1) added in the data layer tab *(Figure 7-3)*. These include the continuous scale for Emission Concentration, and the Aggregate Background Concentration Layer values, provided by the TROPOMI sensor.

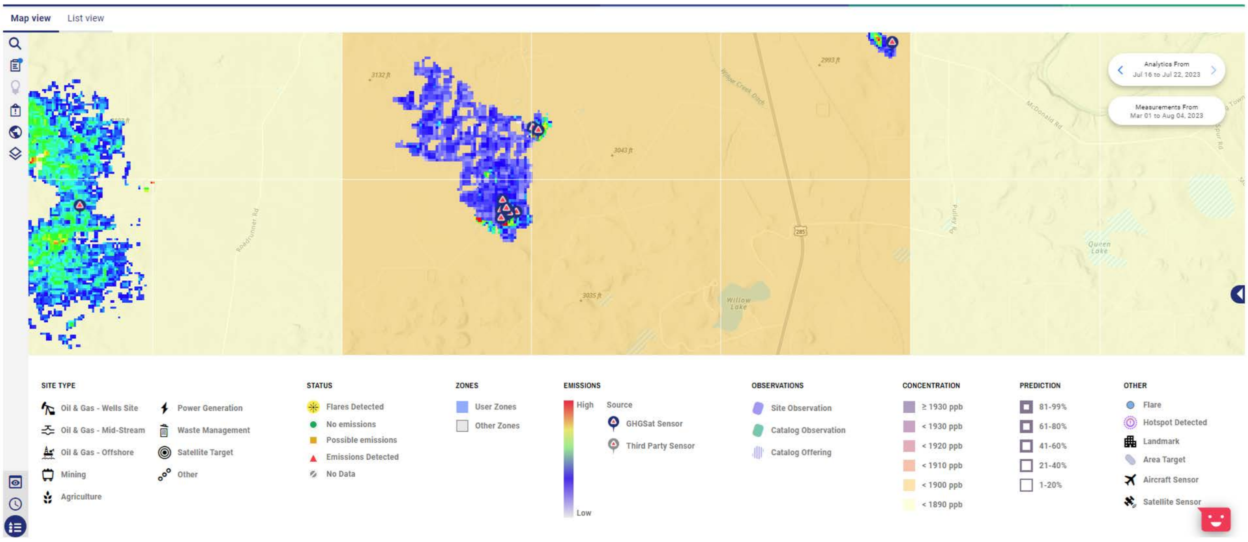

Figure 7-3: *View of the data layer legends available in GHGSat SPECTRA portal. Source: GHGSat*

8. Data download and export

To download data from the SPECTRA portal, users have several options depending on the data and the format they wish to download.

Abundance data

Abundance data provides the methane concentration across the full observation footprint (typically 12 km^2) *(see Figure 7-1)*: Example of GHGSat methane abundance concentration data, display concentration above background (parts per billion volume). Red points indicate location of emission plumes identified within the full image footprint (b). Basemap source Google Maps. These data are available from the Observation List in List View, where each abundance data has a unique observation ID.

To download a single Abundance Product, users should do the following:

- Select the three dots to the right of the product (row) that is required
- Select Download Observations

To download multiple abundance data, users should do the following:

- Select the check box next to required observation IDs
- Select the Download Observations button at the bottom of the page *(see Figure 8-1)*
- From the pop-up window, it is possible to further refine selection by date range (this is optional)
- Select Download Observations to begin data download

Once download has completed, users should do the following:

- Check download folder for zip data download file
- Unzip folder to access each of the observation data packages – these are also contained as .zip files
- Unzip observation files to gain access to abundance data

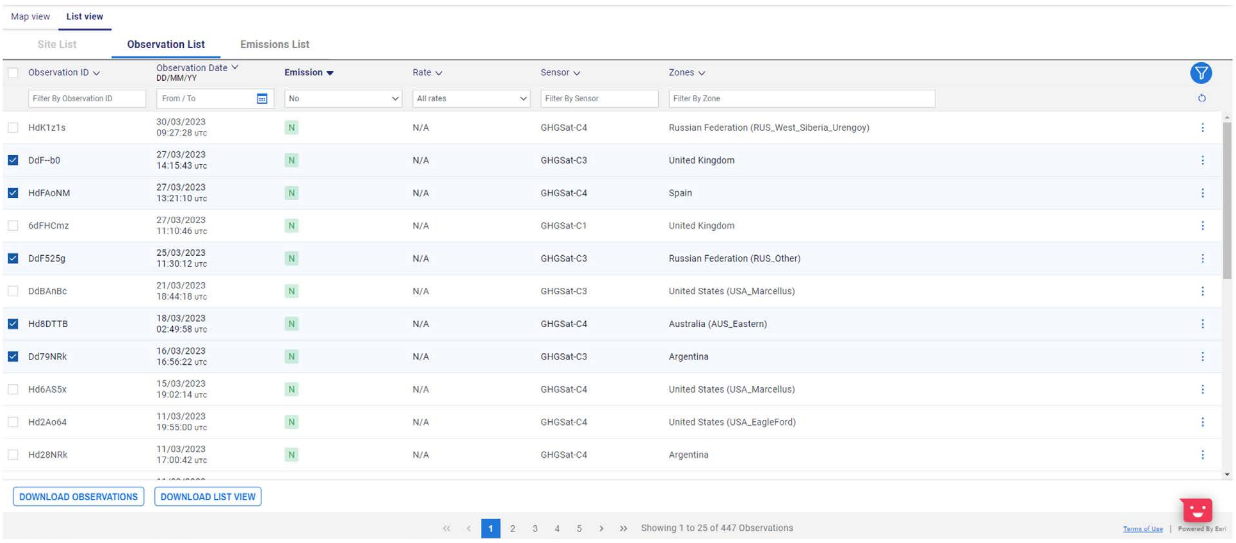

Figure 8-1: *Abundance data download selection from the List View in the SPECTRA data portal.*

Table 8-1: Description of each data product available within an Abundance Data product, shaded rows describe products which are only available where an emission plume is detected.

Suffix	Short Description	Description	Format
ALB	Albedo: Per-pixel short-wave infrared (SWIR) surface reflectance.	The pixel values represent the fraction of light received on a surface that is reflected. A value of zero indicates that no light is reflected and a value of one indicates that all the light received on a surface is reflected.	GeoTIFF
BRW	Reduced resolution albe-do (ALB) and World file	Resolution of the image is reduced compared to the ALB layer. The World file provides reference information for the geographic location of the data.	PNG, WLD
CH_4	Methane concentration measurement (ppb)	The methane concentration values in each pixel represent how many methane particles are in a given volume of air compared to the local background. The background is set to a value of zero. The concentration of the methane particles is measured in parts per billion (ppb) and is a column averaged concentration. The CH_4 GeoTIFF shows methane concentration of the entire observation. Note that the CH_4 GeoTIFF layer can contain artefacts (false positive CH_4 enhancements); enhancements associated to real methane emissions are identified in the CH_4CM PNG and CH_4PL GeoTIFFs.	GeoTIFF
CH_4ER	Methane concentration measurement error (ppb)	Per-pixel CH_4 measurement uncertainty. The uncertainty is for a single satellite pass and includes instrument errors and the quality of the model fitted on the data. The error is defined as the standard deviation.	GeoTIFF
CH_4PL	Methane concentration measurement isolated for each emission plume (ppb)	The CH_4PL GeoTIFF shows the methane concentration reported in the CH_4 layer, only at the location where a plume was detected.	GeoTIFF
CH_4CM	Methane emission plume map	High readability pseudo-colour map combining background imagery and the isolated emission plume identified in the CH_4PL layer.	PNG

FLG	"Flag layer" -- Per-pixel quality designation. Interpretation: (1) Good (2) No data (3) Bad fit	This is a layer that presents the quality of each pixel in CH_4. All the values in the flag layer are 1, 2 or 3: (1) 'Good': The pixel is considered to have good quality data. The values obtained at this location can be trusted. (2) 'No data': There was no data available in the raw data at this location. (3) 'Bad fit': The pixel is considered to have poor quality data. Typically, it means that the error at this location is high and/or that the signal is low. The values obtained at this location cannot always be trusted. They need to be interpreted with caution.	GeoTIFF
CH_4SR	Information about an identified emission (one CSV per plume).	This file includes the spatial coordinates (latitude, longitude), detection time, wind speed, source of the wind information, estimated source rate and uncertainty on the estimated source rate of the plume identified. Each emission has its own ID (_XXXX_CH_4PL), where XXXX is the emission ID. Multiple methane emissions can be detected in one observation. For more information on the source rate and error please see Section 3.	CSV
META	Metadata of the included files. Information about the license, order, observation, and a description of the imagery/data.	This file includes the spatial coordinates (latitude, longitude), detection time, wind speed, source of the wind information, estimated source rate and uncertainty on the estimated source rate of the plume identified. Each emission has its own ID (_XXXX_CH_4PL), where XXXX is the emission ID. Multiple methane emissions can be detected in one observation. For more information on the source rate and error please see Section 3.	JSON

Within each observation folder a number of data products are available (see Table 8-1). The abundance data comes as a .geotiff file, with the suffix ‘CH_4.tif’.
Each file is prefixed with a standard naming convention, which relates to several subfields, separated by underscores, using the following format.

SX_PRODUCTORDER_ACQUISITIONDATE_PROCESSINGDATE_OBSID_SITEID_SUFFIX
where:

- SX: Sensor identifier (D=GHGSAT-D, Cx=GHGSAT-Cx, AVx=Aircraft Variant x)
- PRODUCT ORDER: Internal customer product order number
- ACQUISITION DATE: Observation acquisition date in format “YYYYMMDD”
- PROCESSING DATE: Processing date in format “YYYYMMDD”
- OBS ID: alphanumeric unique observation identifier
- SITE ID: customer site unique numeric identifier (if applicable)
- SUFFIX: file identifier

Emission data

The emission plume datasets are available as a bulk download file, including all available emission plumes from this dataset.

To download these datasets, users should follow these steps:

- Select the Reports selection in the User Profile dropdown *(Figure 8-2)*
- In the subsequent pop-up window, select the download button to begin downloading the bulk data file as .zip file *(Figure. 8-3)*
- Once unzipped, this file includes a separate folder for each satellite observation IDs *(Figure8-4)*
- Within each folder there is a .geotiff file for each of the emission plumes detected in that satellite image
- Additionally, the folder also contains:
    - a .csv file describing the metadata for all emission plumes
    - a QGIS file, with the emission plume sources pre-loaded. This should aid the identification of where and when each of the observation IDs relate to
    - The End User License Agreement (EULA)

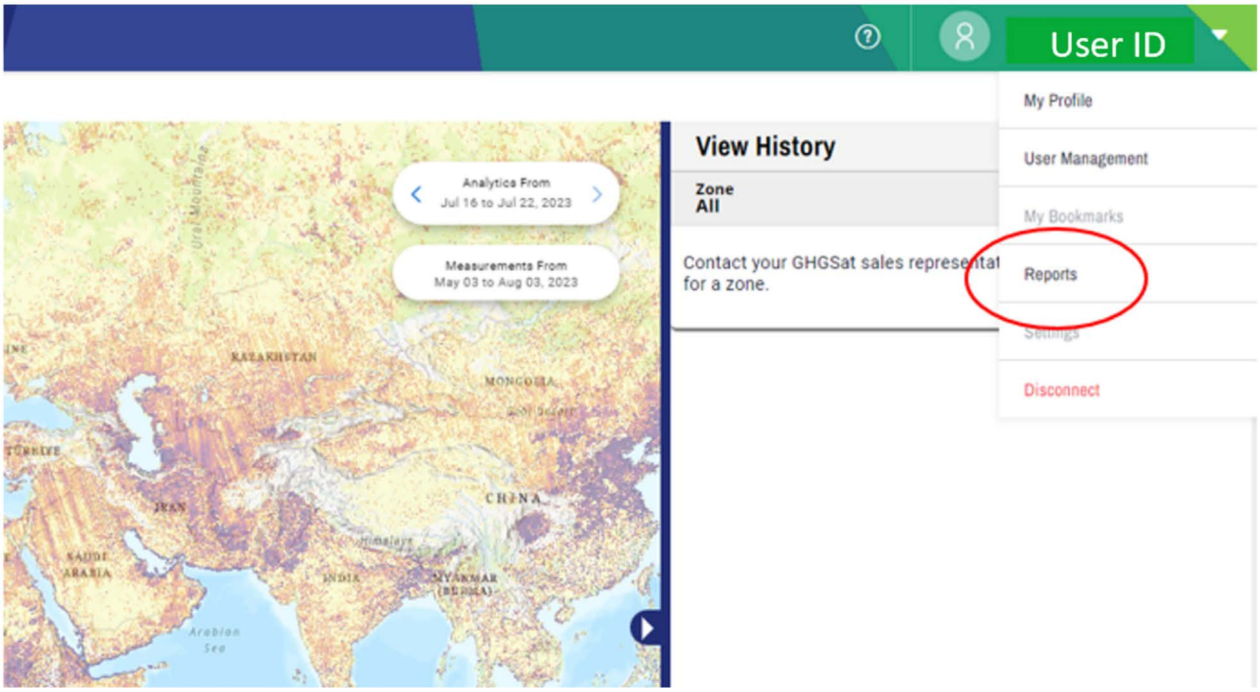

Figure 8-2: Guide to download emission data as a bulk delivery: Finding the Reports folder.

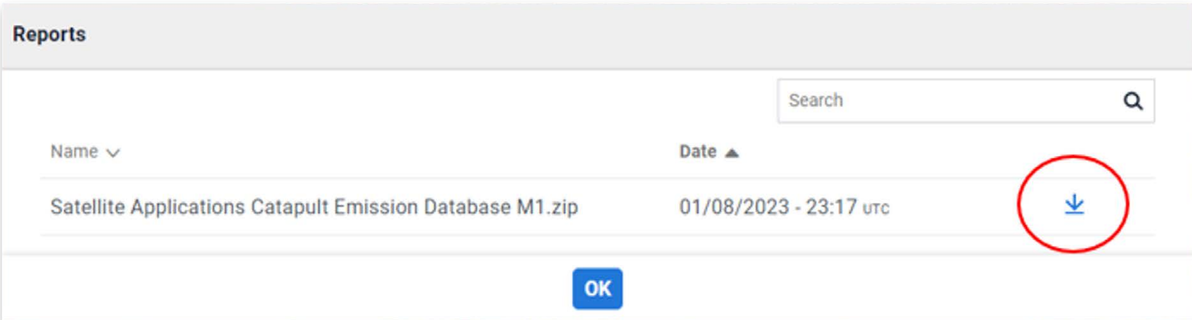

Figure 8-3: Guide to download emission data as a bulk delivery: Download popup file within reports folder.

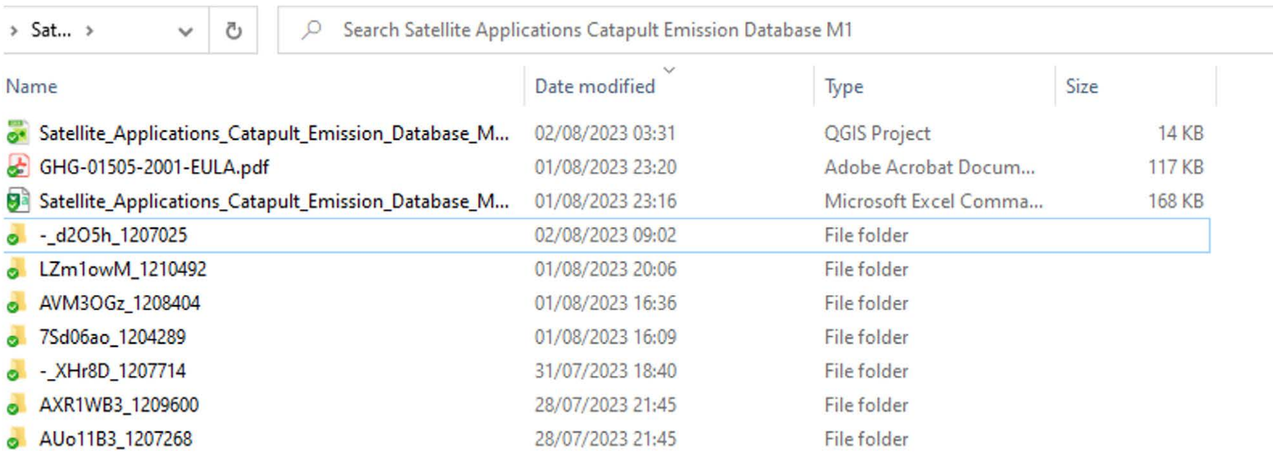

Figure 8-4: Guide to download emission data as a bulk delivery: Listing data available in bulk emission data .zip file.

9. Troubleshooting and support

For further information, please consult the help button within the SPECTRA portal.
Additionally, you can contact either your data consulting organisation (SAC/OS/Defra) or email GHGSat via *success@ghgsat.com*

References

Bai, M., Wang, Z., Lloyd, J., Seneviratne, D., Flesch, T., Yuan, Z. and Chen, D., 2023. Long-term onsite monitoring of a sewage sludge drying pan finds methane emissions consistent with IPCC default emission factor. Water Research X, 19

Brandt, A.R., Heath, G.A. and Cooley, D., 2016. Methane leaks from natural gas systems follow extreme distributions. Environmental science & technology, 50(22)

Chen, D., Chen, A., Hu, X., Li, B., Li, X., Guo, L., Feng, R., Yang, Y. and Fang, X., 2022. Substantial methane emissions from abandoned coal mines in China. Environmental Research, 214

Duren, R.M., Thorpe, A.K., Foster, K.T., Rafiq, T., Hopkins, F.M., Yadav, V., Bue, B.D., Thompson, D.R., Conley, S., Colombi, N.K. and Frankenberg, C., 2019. California's methane super-emitters. Nature, 575(7781), pp.180-184.

Ialongo, I., Stepanova, N., Hakkarainen, J., Virta, H. and Gritsenko, D., 2021. Satellite-based estimates of nitrogen oxide and methane emissions from gas flaring and oil production activities in Sakha Republic, Russia. Atmospheric Environment: X, 11

IPCC, 2023: Sections. In: Climate Change 2023: Synthesis Report. Contribution of Working Groups I, II and III to the Sixth Assessment Report of the Intergovernmental Panel on Climate Change [Core Writing Team, H. Lee and J. Romero (eds.)]. IPCC, Geneva, Switzerland, pp. 35-115

Jervis, D., McKeever, J., Durak, B.O., Sloan, J.J., Gains, D., Varon, D.J., Ramier, A., Strupler, M. and Tarrant, E., 2021. The GHGSat-D imaging spectrometer. Atmospheric Measurement Techniques, 14(3)

Johansson, D.J., Persson, U.M. and Azar, C., 2008. Uncertainty and learning: implications for the trade-off between short-lived and long-lived greenhouse gases. Climatic Change, 88(3-4)

Kozicka, K., Orazalina, Z., Gozdowski, D. and Wójcik-Gront, E., 2023. Evaluation of temporal changes in methane content in the atmosphere for areas with a very high rice concentration based on Sentinel-5P data. Remote Sensing Applications: Society and Environment, 30

Maasakkers, J.D., Varon, D.J., Elfarsdóttir, A., McKeever, J., Jervis, D., Mahapatra, G., Pandey, S., Lorente, A., Borsdorff, T., Foorthuis, L.R. and Schuit, B.J., 2022. Using satellites to uncover large methane emissions from landfills. Science Advances, 8(31)

Myhre, G., D. Shindell, F.-M. Bréon, W. Collins, J. Fuglestvedt, J. Huang, D. Koch, J.-F. Lamarque, D. Lee, B. Mendoza, T. Nakajima, A. Robock, G. Stephens, T. Takemura, and H. Zhang, 2013: Anthropogenic and natural radiative forcing. In Climate Change 2013: The Physical Science Basis. Contribution of Working Group I to the Fifth Assessment Report of the Intergovernmental Panel on Climate Change. T.F. Stocker, D. Qin, G.-K. Plattner, M. Tignor, S.K. Allen, J. Doschung, A. Nauels, Y. Xia, V. Bex, and P.M. Midgley, Eds., Cambridge University Press

Lan, X., Thoning, K.W. and Dlugokencky, E.J., 2023. Trends in globally-averaged CH4, N2O, and SF6 determined from NOAA Global Monitoring Laboratory measurements.

Scheutz, C., Kjeld, A. and Fredenslund, A.M., 2022. Methane emissions from Icelandic landfills–A comparison between measured and modelled emissions. Waste Management, 139

Sherwin, E.D., Rutherford, J.S., Chen, Y., Aminfard, S., Kort, E.A., Jackson, R.B. and Brandt, A.R., 2023. Single-blind validation of space-based point-source detection and quantification of onshore methane emissions. Scientific Reports, 13(1),

Smith, P., Reay, D. and Smith, J., 2021. Agricultural methane emissions and the potential formitigation. Philosophical Transactions of the Royal Society A, 379(2210)

Varon, D.J., Jacob, D.J., McKeever, J., Jervis, D., Durak, B.O., Xia, Y. and Huang, Y., 2018. Quantifying methane point sources from fine-scale satellite observations of atmospheric methane plumes. Atmospheric Measurement Techniques, 11(10)

Vechi, N.T., Mellqvist, J. and Scheutz, C., 2022. Quantification of methane emissions from cattle farms, using the tracer gas dispersion method. Agriculture, Ecosystems & Environment, 330

Wang, S., Liu, Q., Li, J. and Wang, Z., 2021. Methane in wastewater treatment plants: status, characteristics, and bioconversion feasibility by methane oxidizing bacteria for high value-added chemicals production and wastewater treatment. Water Research, 198,

CATAPULT
Satellite Applications

+44 (0) 1235 567999
info@sa.catapult.org.uk
@SatAppsCatapult